Journal of Statistical Physics, Vol. 62, Nos. 1/2, 1991

Interface Interactions in Modulated Phases, and Upsilon Points

Kevin E. Bassler,[1,3] Kazuo Sasaki,[1,2] and Robert B. Griffiths[1]

Received June 12, 1990

Certain features in Frenkel–Kontorova and other models of phases with a one-dimensional modulation can be analyzed by assuming parallel interfaces separating sets of lattice planes belonging to two different phases, and treating the free energy σ to create interfaces, as well as the interaction of two, three, or more interfaces, as phenomenological parameters. A strategy employed by Fisher and Szpilka for interacting defects can be extended to the case of interfaces, allowing a systematic study of the phase diagram by ignoring all interface interactions, and then successively taking into account pair, triple, and higher-order terms. The possible phase diagrams which can occur near the point where $\sigma = 0$ include: various sorts of endpoints analogous to critical endpoints, an accumulation point of first-order transitions and triple points, and a self-similar structure which we call an upsilon point, which turns out to be an accumulation point of an infinite number of segments of first-order transition lines, each of which terminates in two upsilon points.

KEY WORDS: Modulated phases; interfaces; interface interactions; Frenkel–Kontorova models; commensurate–incommensurate transitions.

1. INTRODUCTION

A number of theoretical models have been developed in an attempt to understand the complex structures and phase diagrams of systems which have a modulated structure superimposed on a crystalline lattice.[1–4] Among these are the microscopic ANNNI and chiral clock models,[5,6] phenomenological models based on a Landau expansion,[7,8] and Frenkel–

[1] Department of Physics, Carnegie-Mellon University, Pittsburgh, Pennsylvania 15213.
[2] Permanent address: Department of Engineering Science, Tohoku University, Sendai 980, Japan.
[3] Current address: Department of Materials Science and Engineering, Northwestern University, Evanston, Illinois 60208.

0022-4715/91/0100-0045$06.50/0

Kontorova models.[9–12] Certain features in the phase diagrams of the latter can be conveniently analyzed in terms of a picture of interacting interfaces, which is the subject of this paper.

The Frenkel–Kontorova model, which consists of a set of (classical) atoms in a one-dimensional periodic potential connected with springs, can be regarded as a crude atomic model of a modulated phase or, with somewhat better justification, as a phenomenological model of a three-dimensional system of planes of atoms in which the free energy depends on the average value of an order parameter in each plane. A number of studies, mainly by Aubry and his collaborators,[9–11] have shown that the ground states of a Frenkel–Kontorova model (which correspond to the minimum free energy, or equilibrium state of the corresponding three-dimensional system) can exhibit an infinite set of periodic and quasiperiodic phases with a complicated but continuous series of commensurate–incommensurate transitions as a suitable parameter is varied. A useful way of thinking about these transitions is in terms of a set of interacting defects ("discommensurations," "kinks," or "solitons") whose creation energy is a function of the thermodynamic parameters in the system.

Numerical studies[13,14] have shown that the addition of suitable harmonics (even with an extremely small amplitude) to the cosine potential of the standard Frenkel–Kontorova model can give rise to first-order transitions terminating in a complicated sort of "multicritical" point where the surface tension σ between the coexisting phases goes to zero. In the phase diagram one finds a fan-shaped structure consisting of a complicated mixture of different phase transitions emerging on the side of this multicritical point where σ is negative, opposite the first-order phase transition. Because the sides of the fan come together at a cusp which is tangential to the first-order transition, resembling the Greek letter Υ, we shall refer to this multicritical point as an *upsilon point.* Upsilon points also occur in certain Frenkel–Kontorova models with a nonconvex interaction ("spring") potential between atoms[15] and in an exactly soluble model of Aubry *et al.*[16]

In this paper we shall show that upsilon points can be discussed in terms of interacting interfaces in much the same way that commensurate–incommensurate transitions can be discussed in terms of interacting defects. If an upsilon point occurs at the end of a first-order transition separating phases α and β, then the modulated structures of interest consist of a certain number of planes of phase α, followed by planes of phase β, followed by more planes of α, and so forth, with interfaces occurring at each transition from one phase to the other. The equilibrium (minimum free energy) states of such a system can be worked out using a set of phenomenological parameters: the free energies of phases α and β, the free

energy σ to create an interface, which may be positive or negative, and the energies of interactions of two or more interfaces, which may be of either sign. Depending on the signs of these interactions, an upsilon point or some other structure will arise at the end of the first-order transition line.

The strategy we use in studying the phase diagram involves an extension of the method of Fisher and Szpilka,[17] which they used for studying interacting defects, to the case of interacting interfaces. Thus, following Section 2, which introduces the notation for the interacting interfaces model, we consider in Section 3 the phase diagram when all the interactions among interfaces have been turned off. The pair interactions are turned back on in Section 4, and the three-interface interactions in Section 5. At each stage we find a phase diagram containing first-order lines and superdegenerate lines or points, and we assume that the former will be left qualitatively unchanged, while the latter will be further split or transformed into first-order transitions by the remaining higher-order interactions, which are always assumed to be small relative to those already considered. The effects of four-interface and higher-order interactions upon the phase diagrams obtained in Section 5 are discussed using a "renormalization" approach applied to certain superdegenerate lines in Section 6 and to a class of superdegenerate points in Section 7. Then the effects of all remaining interactions can, at least in favorable cases, be determined by iterative procedures. The process is carried out in some detail in Section 8 using the "exponential interactions" which Sasaki has shown[18] are to be expected under fairly general conditions in the case of the interfaces arising in Frenkel–Kontorova models, provided they are widely separated. The upsilon point turns out to be self-similar in the sense that an infinite number of short segments of first-order lines occurs in its neighborhood, and each of these segments terminates in two upsilon points. Our conclusions are summarized in Section 9.

2. INTERFACES AND THEIR INTERACTIONS

We suppose that the system of interest to us consists of a number of parallel planes of atoms (spins, or whatever), and that each plane belongs to one of two phases, α and β, or lies near an interface between these phases. Phase α is assumed to be periodic with period $Q_\alpha \geqslant 1$; that is, planes n and $n+Q_\alpha$ (if not near an interface) are identical in terms of their average thermal properties, whereas planes n and $n+1$ are different, unless $Q_\alpha = 1$. Similarly, we assume that phase β is periodic with period $Q_\beta \geqslant 1$.

As for planes lying near an interface, we assume that some convention has been adopted, applicable to all interfaces of this type, whereby the center of the interface is assigned a position midway between two planes.

Then all planes lying on the α side of this interface, in a region extending to the next interface, are, by convention, assigned to phase α, and those on the β side to phase β. Consequently, the system can be thought of as containing l_1 planes of phase α, followed by m_1 planes of phase β, followed by l_2 planes of phase α, and so forth, with the total number N of planes in the system equal to the sum of the l's and the m's. We assume that the free energy H of the system as a whole is some function of the *configuration* $\{l_i, m_i\}$ of l's and m's, the set of numbers giving the number of planes separating adjacent interfaces.

In addition, we assume that the number of planes l associated with a segment of phase α lying between adjacent interfaces is not arbitrary, but can only take on the values

$$l = l^* + pQ_\alpha \tag{2.1}$$

where l^* is a fixed positive number giving the minimum value of the length of such a segment, and $p \geqslant 0$ is any nonnegative integer. Similarly, the number of planes m in a segment of β can only take the values

$$m = m^* + qQ_\beta \tag{2.2}$$

with $m^* > 0$ fixed, and $q \geqslant 0$ arbitrary.

While the restrictions (2.1) and (2.2) may at first seem surprising, they are not unreasonable. To begin with, we are not totally excluding other possibilities, but only assuming that their free energies are significantly higher, and hence they can be ignored when studying the equilibrium state, the state of minimal free energy. Next, given two phases α and β, there may well be a number of possible interfaces between them, but one of these is likely to have a lower free energy than the others, and for simplicity we assume that only this type occurs in the equilibrium state. (We allow for the possibility that the α-followed-by-β or α–β interface is distinct from the β–α interface, so as to allow for phases which lack a mirror symmetry, but we assume that just one interface of each type occurs.) Now if phase α has a period $Q_\alpha > 1$, it is plausible that the position of the minimum-free-energy β–α interface relative to a plane of a particular type in phase α should be a definite number modulo Q_α. Considerations of this sort suggest (2.1) and (2.2); they may also, of course, simply be regarded as part of the definitions of our model.

The foregoing terminology is easily adapted to a Frenkel–Kontorova model of a one-dimensional array of atoms in a periodic potential. One speaks of individual atoms, not planes, assigned to phases α and β, with l_i and m_i the numbers of atoms in the corresponding segments of α and β. If x_n is the position of the nth atom and the periodic potential has a period

a, then a periodic phase of period $Q > 0$ is one for which there is an integer P such that

$$x_{n+Q} = x_n + Pa \tag{2.3}$$

for all n, and Q is the smallest positive integer for which this relation holds. Naturally, it is this Q which enters (2.1) or (2.2), as the case may be. In the Frenkel–Kontorova case, H is the energy, and we are interested in the minimum energy or ground state. Consequently, in what follows we shall sometimes use "ground state" to refer to the equilibrium state of minimum free energy.

Although both α and β are assumed to be periodic, the actual configuration (of planes or atoms) may be periodic or not, depending on the set of integers $\{l_i, m_i\}$. The following is a convenient notation for periodic configurations. Let $[lm]$ denote the configuration in which $l_i = l$ and $m_i = m$ for all i, $[lml'm']$ that in which $l_i = l$ and $m_i = m$ for i even, and $l_i = l'$, $m_i = m'$ for i odd, and so forth: the letters between brackets denote a segment whose repetition generates the entire configuration.

Free energies are assigned to configurations $\{l_i, m_i\}$ in the following way. Let ε_α and ε_β be the free energy per plane (energy per atom in a Frenkel–Kontorova model) in the pure phases α and β, respectively, when no interfaces are present. Next consider the situation in Fig. 1, where (a) and (b) are schematic representations of two systems containing an equal number of planes, with m planes of phase α in (a) changed to phase β in (b). The difference in free energies is then

$$\Delta H = H^{(b)} - H^{(a)} = (\varepsilon_\beta - \varepsilon_\alpha)m + 2\sigma + \phi_\beta(m) \tag{2.4}$$

where 2σ is the free energy required to create two interfaces, and $\phi_\beta(m)$ is the interaction free energy of these interfaces when separated by m planes. We require that $\phi_\beta(m)$ go to zero as m becomes large, always assuming

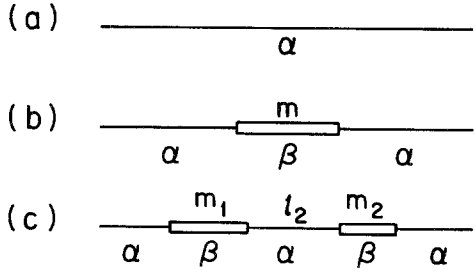

Fig. 1. Diagram showing how interface creation and interaction free energies can be computed by inserting segments of one phase into another.

that m is very small compared to the total number of planes, and hence σ may be defined by a limiting process:

$$2\sigma = \lim_{m \to \infty} [\Delta H - (\varepsilon_\beta - \varepsilon_\alpha)m] \tag{2.5}$$

Consequently, one can regard (2.4) as defining $\phi_\beta(m)$, for a fixed m, as ΔH minus the first two terms on the right-hand side.

A similar procedure can be used to define $\phi_\alpha(l)$, the interaction of two interfaces separated by l planes of phase α, and also three-interface and four-interface interactions, etc. Thus, for example, Fig. 1c shows a configuration whose free energy relative to that of Fig. 1a is given by

$$\begin{aligned}\Delta H = {} & (\varepsilon_\beta - \varepsilon_\alpha)(m_1 + m_2) + 4\sigma + \phi_\beta(m_1) + \phi_\alpha(l_2) \\ & + \phi_\beta(m_2) + \phi_\beta(m_1, l_2) + \phi_\alpha(l_2, m_2) + \phi_\beta(m_1, l_2, m_2)\end{aligned} \tag{2.6}$$

In this expression a ϕ_α or ϕ_β with n arguments represents the interaction of $n+1$ interfaces. The subscript denotes the phase corresponding to the first argument. Note that the only two-interface terms in (2.6) correspond to adjacent interfaces; an interaction between the first and third interfaces in Fig. 1c can be incorporated in the three-interface term $\phi_\beta(m_1, l_2)$. A similar comment applies to higher-order interactions: the interfaces involved are always consecutive. We always assume that ϕ_α or ϕ_β goes to zero as any one of its arguments goes to infinity. This makes it possible to define various n-interface interactions by means of appropriate limiting processes and subtractions, as in (2.5) and the remarks which follow.

An equivalent approach to defining or calculating interface interaction energies makes use of *reconnection* formulas,[19] as in Fig. 2. The configurations (a) and (b) are obtained by "reconnecting" (c) and (d) in the following

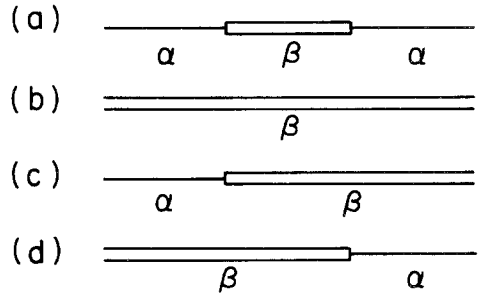

Fig. 2. Diagram illustrating the calculation of interface pair interactions by means of a reconnection formula, Eq. (2.7).

sense. If (c) and (d) are "broken" at the position of the interface in (d), and the planes following this interface in (c) are interchanged with the corresponding planes in (d), the result is that (*c*) is transformed into (a) and (d) into (b). What makes this procedure useful is the formula

$$\phi_\beta(m) = H^{(a)} + H^{(b)} - H^{(c)} - H^{(d)} \tag{2.7}$$

which expresses the interface interaction free energy in terms of the free energies of the four configurations shown in the figure; that is, in terms of the work required to accomplish the reconnection.

Note that the configurations (c) and (d) in Fig. 2 do not have to have the same number of planes, and might have various type of boundary condition at either end. Formula (2.7) remains valid provided configurations (a) and (b), and their boundary conditions, are consistent with their having been obtained by reconnecting (c) and (d). (Of course, the boundaries must be far enough away so that they have a negligible interaction with the interfaces shown in the figure.)

The same reconnection procedure works for multiple interface interactions. Thus one has

$$\phi_\alpha(l_1, m_1, l_2, m_2) = H^{(a)} + H^{(b)} - H^{(c)} - H^{(d)} \tag{2.8}$$

for the configurations of Fig. 3. In the general case, configuration (a) contains precisely those interfaces whose interaction one wishes to evaluate. Then (d), (c), and (b) are obtained by eliminating the leftmost, the rightmost, and both extreme interfaces, respectively, from (a), in a manner which leaves the planes between the extreme interfaces in (a) unaltered.

In light of the preceding discussion, we shall assume that the free energy of a general configuration $\{l_i, m_i\}$ is of the form

$$H = \sum_{i=1}^{\nu} (2\sigma + l_i\varepsilon_\alpha + m_i\varepsilon_\beta) + \Phi \tag{2.9}$$

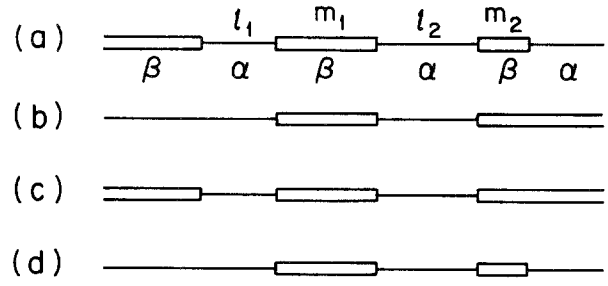

Fig. 3. Diagram illustrating the calculation of a five-interface interaction by means of a reconnection formula, Eq. (2.8).

where

$$\Phi = \sum_{i=1}^{v} [\phi_\alpha(l_i) + \phi_\beta(m_i) + \phi_\alpha(l_i, m_i) + \phi_\beta(m_i, l_{i+1}) + \phi_\alpha(l_i, m_i, l_{i+1}) + \cdots] \tag{2.10}$$

is the sum of the interactions of the $2v$ interfaces. The total number of planes is given by

$$N = \sum_{i=1}^{v} (l_i + m_i) \tag{2.11}$$

The subscript α or β on a ϕ denotes the phase corresponding to the first argument, and is hence redundant if the argument itself indicates which phase is involved. Since we shall always use l's for phase α and m's for phase β, the subscript will sometimes be dropped, and also the commas separating arguments. Thus, for example, $\phi(mlm\bar{l})$ denotes $\phi_\beta(m, l, m, \bar{l})$.

Equations (2.9)–(2.11), along with the conditions (2.1) and (2.2), constitute the definition of the interface model whose phase diagram will be studied in the remainder of this paper by minimizing the free energy per plane,

$$f = H/N \tag{2.12}$$

as a function of various parameters in H. Since adding a constant to both ε_α and ε_β does not influence the relative free energies of different phases, it is convenient to use the parameter

$$\varepsilon = \varepsilon_\alpha - \varepsilon_\beta \tag{2.13}$$

in constructing phase diagrams, in place of the two parameters ε_α and ε_β.

We shall be interested in phase diagrams in the σ, ε plane in the vicinity of the origin where σ and ε vanish. In applications of the interface model, σ and ε can be regarded as smooth functions of thermodynamic field variables (such as temperature, pressure, chemical potentials), or of the parameters (temperature, exchange constants, etc.) of a microscopic or phenomenological model. The same is true of the various ϕ's.

Rather than minimizing H/N, it is sometimes more convenient to minimize

$$\mathcal{H} = H - fN = 2\sigma v + \mathcal{H}_0 \tag{2.14}$$

with f and v held fixed, and N allowed to vary. Equivalently, one may minimize

$$\mathcal{H}_0 = \sum_{i}^{v} (l_i \eta_\alpha + m_i \eta_\beta) + \Phi \tag{2.15}$$

with

$$\eta_\alpha = \varepsilon_\alpha - f, \qquad \eta_\beta = \varepsilon_\beta - f \tag{2.16}$$

and v held fixed. As shown in Appendix A, the (unique) value of f for which $\mathscr{H} = 0$ is the desired minimum of (2.12), and consequently, for this f,

$$-2\sigma = \min(\mathscr{H}_0)/v \tag{2.17}$$

One can think of $\mathscr{H}_0$ as a "lattice Hamiltonian" for "spin variables" l_i and m_i defined on a one-dimensional lattice of unit cells indexed by i, with two sites per unit cell. From this perspective, $l_i\eta_\alpha + \phi_\alpha(l_i)$ is a single-site energy, $\phi_\alpha(l_i, m_i)$ a nearest-neighbor interaction, etc.

3. APPROXIMATION OF NONINTERACTING INTERFACES

Our analysis of the model introduced in Section 2 begins with the approximation of noninteracting interfaces: Φ is set equal to zero in (2.9). To be specific, consider a case in which $l^* = 3$, $Q_\alpha = 2$, $m^* = 2$, and $Q_\beta = 3$. Then any configuration consistent with (2.1) and (2.2) corresponds to a walk on the *energy graph* shown in Fig. 4a, following the directed edges in the direction of the arrows, with successive vertices representing planes of type α or β. The total free energy (2.9) is a sum of weights ε_α and ε_β associated with the α and β vertices, and σ for each of the horizontal edges, corresponding to the α–β and β–α interfaces.

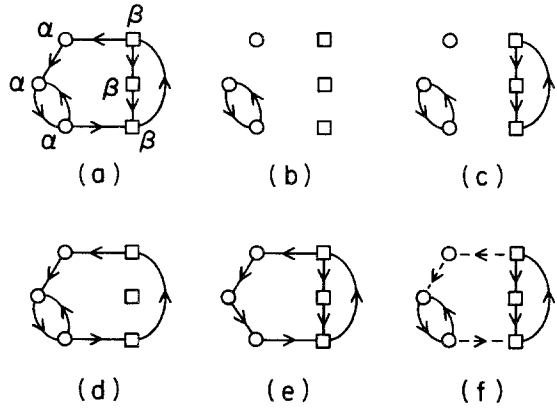

Fig. 4. (a) Energy graph and (b)–(c) various ground state graphs, for $l^* = 3$, $q_\alpha = 2$, $m^* = 2$, $Q_\beta = 3$. In (f) the dashed edges are those needed when inserting a segment of α into β or vice versa.

Any periodic configuration is associated with a cycle on this graph, and its free energy per plane is the *cyclic average*: the total weight for the cycle divided by its length. The minimum cyclic average is the equilibrium or "ground state" free energy, and we call the corresponding cycle (which need not be unique) a *periodic ground state*. There is always some minimizing cycle for any choice of the parameters in H.

The *ground state graph* is defined as that subgraph of the energy graph which contains all edges belonging to a periodic ground state. Several possibilities are shown in Fig. 4. In Fig. 4b there is a simple cycle of length two corresponding to phase α, while in Fig. 4c the ground state is degenerate: α and β have the same free energy per plane. In such a case, when the cycles are disjoint with no common vertices, we shall say that these phases coexist at a *first-order* transition. By contrast, the connected graph in Fig. 4d is a *superdegenerate* ground state because any walk on this graph yields the same free energy per plane, and the number of possible distinct walks of a given length increases exponentially with the length (corresponding to a finite entropy), due to the fact that at the lowest α vertex there are two possibilities for the next step. Another superdegenerate ground state is shown in Fig. 4e.

The distinction between first-order and superdegenerate is very important for our analysis of phase diagrams. Arbitrarily weak perturbations due to terms which have been omitted from the analysis can split a superdegenerate point or line on the phase diagram in such a way as to reveal several distinct configurations (possibly an infinite number), each stable for an appropriate choice of the relevant parameters. By contrast, at a first-order coexistence, additional perturbations, if they are sufficiently weak, can create no new stable phases, and thus their effect will be to produce small quantitative changes in the phase diagram—shifts in the positions of points or lines—rather than qualitatively new features.

It is typical of first-order coexistence that it costs a finite amount of free energy to insert a segment of one phase into another (as in Fig. 1b), corresponding to a positive surface tension. This is evident in the case of $\alpha:\beta$ coexistence in Fig. 4c, because such an insertion corresponds to a walk making use of edges—shown dashed in Fig. 4f—which are not part of any ground state. In this instance one can compute the additional free energy and show that it is 2σ, as expected. By contrast, if the ground state graph is connected, as in the superdegenerate cases of Figs. 4d and 4e, there is obviously no additional free energy cost to insert a segment of one phase in the other, so the surface tension is zero.

Whatever the values of l^*, Q_α, m^*, and Q_β, the energy graph always contains three simple (no repetition of vertices) cycles corresponding to phases α, β, and $[l^*m^*]$. A comparison of their free energies yields the

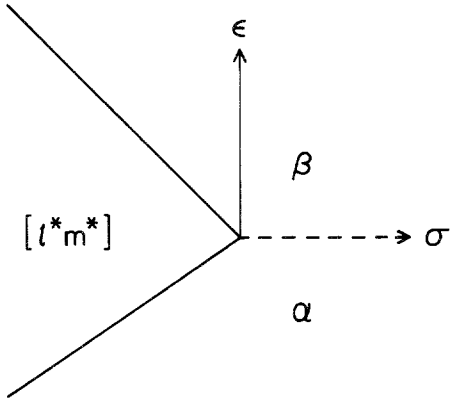

Fig. 5. Phase diagram in the σ, ε plane for noninteracting interfaces. The slopes of the solid lines depend on l^* and m^*.

phase diagram of Fig. 5 in the σ, ε plane ($\varepsilon = \varepsilon_\alpha - \varepsilon_\beta$). The dashed line at $\varepsilon = 0$, $\sigma > 0$ represents the first-order coexistence of α and β, whereas the solid lines

$$\varepsilon = 2\sigma/m^* \tag{3.1}$$

$$\varepsilon = -2\sigma/l^* \tag{3.2}$$

for $\sigma < 0$ are superdegenerate lines, corresponding to Figs. 4d and 4e, separating the *mixed-phase region* (occupied by $[l^*m^*]$ in this approximation) from phases α and β, respectively. We shall next study how these superdegenerate lines are modified by interface interactions.

4. PAIR INTERACTION APPROXIMATION

In the pair approximation, the terms $\phi_\alpha(l)$ and $\phi_\beta(m)$ involving interactions of pairs of interfaces are retained in (2.10), but all the ϕ's with two or more arguments, corresponding to the interaction of three or more interfaces, are set equal to zero. As a consequence, (2.9) can be written in the form

$$H = \sum_i (l_i + m_i) f(l_i, m_i) \tag{4.1}$$

where

$$f(l, m) = [2\sigma + \varepsilon_\alpha l + \varepsilon_\beta m + \phi_\alpha(l) + \phi_\beta(m)]/(l + m) \tag{4.2}$$

is the free energy per plane for the periodic phase $[lm]$. If f has a unique minimum at $l=\bar{l}$, $m=\bar{m}$, the inequality

$$H/N - f(\bar{l}, \bar{m}) = N^{-1} \sum_i (l_i + m_i)[f(l_i, m_i) - f(\bar{l}, \bar{m})] \geqslant 0 \tag{4.3}$$

tells us that $[\bar{l}\bar{m}]$ is the unique equilibrium or ground state, since any other configuration will have a higher free energy per plane. On the other hand, if f achieves its minimum at two (or more) choices of (l, m), the equilibrium state is superdegenerate, since each (l_i, m_i) can take on either of these two values.

A geometrical construction of the type considered by Fisher and Szpilka[17] is useful for visualizing the process of finding the minimum of $f(l, m)$. Construct graphs of $\phi_\alpha(l)$ and $\phi_\beta(m)$, Figs. 6a and 6b, consisting of discrete points at the values of l and m allowed by (2.1) and (2.2). If through the points $(l, \phi_\alpha(l))$ and $(m, \phi_\beta(m))$ straight lines are drawn with slopes $-\eta_\alpha$ and $-\eta_\beta$, respectively, their intersections with the vertical axes occur at

$$s_\alpha = \phi_\alpha(l) + l\eta_\alpha, \qquad s_\beta = \phi_\beta(m) + m\eta_\beta \tag{4.4}$$

Upon making the identifications [consistent with (2.16)]

$$\varepsilon_\alpha = \eta_\alpha + f, \qquad \varepsilon_\beta = \eta_\beta + f \tag{4.5}$$

and

$$\sigma = -\tfrac{1}{2}(s_\alpha + s_\beta) \tag{4.6}$$

we recover (4.2).

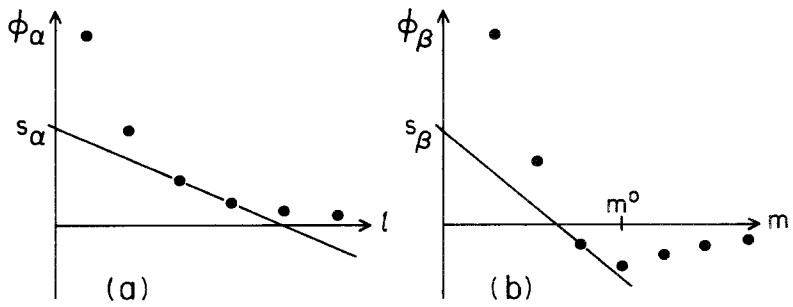

Fig. 6. Graphs of (a) $\phi_\alpha(l)$, (b) $\phi_\beta(m)$ showing lower tangent lines and their intersections with the ϕ axes.

We shall call one of these straight lines a *lower tangent line* if it lies below, or passes through, every other point on the graph. The examples in Fig. 6 have this character. It is obvious that for a given η_α, s_α in (4.4) takes on its minimum value when the straight line is a lower tangent line; and similarly s_β for a given η_β. Consequently, in view of (4.6), σ is maximized for a specified f and ε (and thus a specified η_α and η_β) by that l and that m through which the corresponding lower tangent lines pass. (Of course, the l and m may not be unique, as, for example, in Fig. 6a.) It is also the case that for this ε and σ, the same l and m minimize f in (4.2). For suppose there were some other values l', m' yielding as

$$f' = \frac{2\sigma + l'\varepsilon_\alpha + m'\varepsilon_\beta + \phi_\alpha(l') + \phi_\beta(m')}{l' + m'} \tag{4.7}$$

strictly less than f. We could then increase σ in (4.7) until f' was equal to our previous f (note that $l' + m'$ is positive). This would be a contradiction, as the new value of σ would exceed the previous value, which was, by hypothesis, a maximum.

As a first application of the geometrical construction, note that if, say, $\phi_\beta(m)$ has a unique negative minimum at $m = m^\circ$, as in Fig. 6b, the fact that $\phi_\beta(m)$ tends to zero as m becomes infinite implies that no $m > m^\circ$ can ever appear in an equilibrium or ground state, as it is impossible to pass a lower tangent line through $(m, \phi_\beta(m))$. Analogous remarks apply to ϕ_α. By contrast, if ϕ_α and ϕ_β satisfy the convexity conditions

$$\Delta^2\phi_\alpha(l) = \phi_\alpha(l + Q_\alpha) + \phi_\alpha(l - Q_\alpha) - 2\phi_\alpha(l) > 0 \tag{4.8}$$

$$\Delta^2\phi_\beta(m) = \phi_\beta(m + Q_\beta) + \phi_\beta(m - Q_\beta) - 2\phi_\beta(m) > 0 \tag{4.9}$$

for all $l > l^*$ and $m > m^*$, respectively, then every l and m allowed by (2.1) and (2.2) will appear in the phase diagram.

Although it is not essential to our analysis, a convenient assumption, which will simplify the exposition below, is that ϕ_α and ϕ_β are *initially convex* in the following sense: Either ϕ_α is everywhere positive and (4.8) holds for all allowed $l > l^*$, or else it has a unique negative minimum at $l = l^\circ$, and (4.8) holds for $l^* < l < l^\circ$. Similarly, for ϕ_β, (4.9) holds for all allowed m in the range $m^* < m < m^\circ$, where m° is either the unique negative minimum of ϕ_β, or $+\infty$ in the case in which ϕ_β is everywhere positive. Assuming initial convexity, it is helpful to distinguish three cases:

A. ϕ_α and ϕ_β everywhere positive.

B. Either ϕ_α and ϕ_β has a negative minimum, and the other is everywhere positive.

C. Both ϕ_α and ϕ_β have negative minima.

Given that ϕ_α is initially convex, a lower tangent line either passes through a single point of the graph, in which case its slope can be varied within certain limits, or it passes through two successive points, say l and $\bar{l}$, in which case its slope is $-\eta_\alpha$ with

$$\eta_\alpha[\phi_\alpha(l)-\phi_\alpha(\bar{l})]/(\bar{l}-l) \tag{4.10}$$

and its intercept with the vertical axis is

$$s_\alpha=\phi_\alpha(l)+l\eta_\alpha=\phi_\alpha(\bar{l})+\bar{l}\eta_\alpha \tag{4.11a}$$

or

$$s_\alpha=[\bar{l}\phi_\alpha(l)-l\phi_\alpha(\bar{l})]/(\bar{l}-l) \tag{4.11b}$$

The corresponding formulas for ϕ_β are

$$\eta_\beta=[\phi_\beta(m)-\phi_\beta(\bar{m})]/(\bar{m}-m) \tag{4.12}$$

$$s_\beta=\phi_\beta(m)+m\eta_\beta=\phi_\beta(\bar{m})+\bar{m}\eta_\beta \tag{4.13a}$$

or

$$s_\beta=[\bar{m}\phi_\beta(m)-m\phi_\beta(\bar{m})]/(\bar{m}-m) \tag{4.13b}$$

The discussion following (4.3) shows that either (4.10) or (4.12) gives rise to a superdegenerate ground state. Consequently, the positive quadrant of the η_α, η_β plane (note that η_α and η_β cannot be negative, for a lower tangent line cannot have a positive slope) is divided into a set of rectangles, as shown in Fig. 7, by superdegenerate lines. In each rectangle there is a

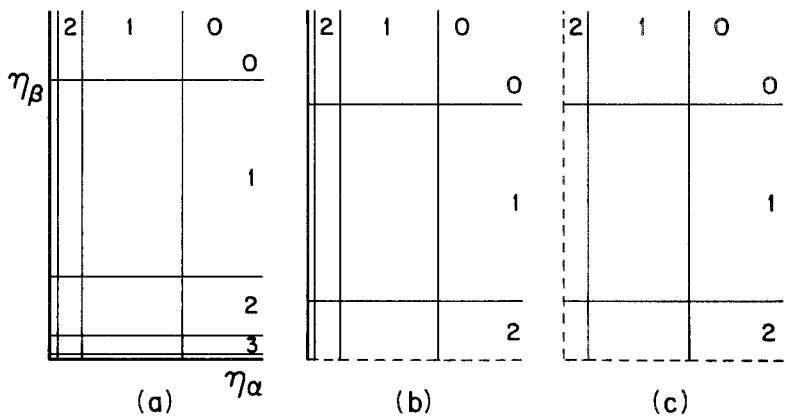

Fig. 7. Phase diagram in the positive η_α, η_β quadrant for (a) case A, (b) case B, (c) case C. The numbers at the top of each figure give the value of p, and those at the right side the values of q (see rext).

single simple mixed phase $[lm]$, where l is given by (2.1) using the p value indicated above the rectangle at the top of the figure, and m by (2.2) using the q value indicated to the right of the rectangle. Cases A, B, and C correspond to 7a, 7b, and 7c: an infinite number of superdegenerate lines parallel to both axes, an infinite number parallel to one and a finite number parallel to the other, or only a finite number of superdegenerate lines parallel to both axes. The heavy lines indicate the axes which are accumulations of superdegenerate lines.

The various features in the positive η_α, η_β quadrant can be mapped into the σ, ε plane by inserting (4.10)–(4.13) in (4.5) and (4.6), and using (2.13):

$$\varepsilon = \varepsilon_\alpha - \varepsilon_\beta = \eta_\alpha - \eta_\beta \tag{4.14}$$

The result is a set of parallelograms, as in Fig. 8, formed by straight lines connecting the four phase points, located at

$$\sigma = \frac{1}{2}\left\{\frac{l\phi_\alpha(\bar{l}) - \bar{l}\phi_\alpha(l)}{\bar{l}-l} + \frac{m\phi_\beta(\bar{m}) - \bar{m}\phi_\beta(m)}{\bar{m}-m}\right\} \tag{4.15}$$

$$\varepsilon = \left(\frac{\phi_\alpha(l) - \phi_\alpha(\bar{l})}{\bar{l}-l}\right) - \left(\frac{\phi_\beta(m) - \phi_\beta(\bar{m})}{\bar{m}-m}\right) \tag{4.16}$$

where the phases $[lm]$, $[l\bar{m}]$, $[\bar{l}m]$, and $[\bar{l}\bar{m}]$ come together.

The phase diagram for case A (ϕ_α and ϕ_β both positive), shown in Fig. 8, can be analyzed in the following way. The geometrical construction implies that s_α and s_β are positive, so σ must be negative whenever mixed phases are present. Thus, for $\sigma > 0$ the only possible phases are α and β; the

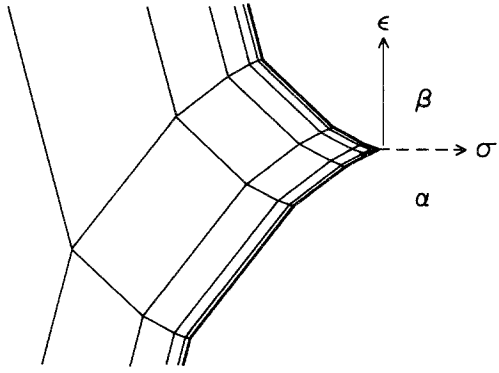

Fig. 8. Phase diagram for case A in the σ, ε plane.

former minimizes f for $\varepsilon < 0$ and the latter for $\varepsilon > 0$. Thus, at $\varepsilon = 0$ there is a first-order phase boundary with a positive interface-creation free energy, as noted above in Section 3.

The convexity conditions (4.8) and (4.9) along with the positivity of ϕ_α and ϕ_β imply that all simple mixed phases $[lm]$ with l and m given by (2.1) and (2.2) actually occur in the phase diagram. The general appearance of the mixed-phase region is that shown in Fig. 8: a wedge with piecewise linear boundaries separating it from phases α and β. (Note that this and subsequent figures have been constructed using specific choices for ϕ_α and ϕ_β; however, the topological structure will be the same for any other convex choice.)

To locate the boundary between phase α and the mixed-phase region, let m be fixed and take the limit as l becomes infinite in the geometrical construction. Then both η_α and s_α tend to zero, so that $\eta_\beta = -\varepsilon$ and $s_\beta = -2\sigma$ from (4.14) and (4.6). Consequently, from (4.4),

$$2\sigma + \phi_\beta(m) - m\varepsilon = 0 \tag{4.17}$$

where m is that value which for a given ε $(= -\eta_\beta)$ minimizes $\phi_\beta(m) - m\varepsilon$ $(= s_\beta)$. Since m changes in discrete steps as ε varies, the boundary consists of a set of straight-line segments. The point at which the segment associated with m intersects that associated with $\bar{m} = m + Q_\beta$ is obtained by letting l and $\bar{l}$ tend to infinity in (4.15) and (4.16):

$$\begin{aligned} \sigma &= [m\phi_\beta(\bar{m}) - \bar{m}\phi_\beta(m)]/2(\bar{m} - m) \\ \varepsilon &= -[\phi_\beta(m) - \phi_\beta(\bar{m})]/(\bar{m} - m) \end{aligned} \tag{4.18}$$

The slope of these segments, $\Delta\varepsilon/\Delta\sigma$, tends to zero as m tends to infinity and ε increases to zero.

Precisely the same analysis, with l held fixed and m tending to infinity, yields the formula

$$2\sigma + \phi_\alpha(l) + \varepsilon l = 0 \tag{4.19}$$

for the boundary between phase β and the mixed-phase region, with l in (4.19) the value which minimizes $\phi_\alpha(l) + \varepsilon l$ for a given ε. The boundary consists of straight-line segments, with the l and $\bar{l} = l + Q_\alpha$ segments intersecting at

$$\begin{aligned} \sigma &= [l\phi_\alpha(\bar{l}) - \bar{l}\phi_\alpha(l)]/2(\bar{l} - l) \\ \varepsilon &= [\phi_\alpha(l) - \phi_\alpha(\bar{l})]/(\bar{l} - l) \end{aligned} \tag{4.20}$$

Once again, the slope $\Delta\varepsilon/\Delta\sigma$ of these segments tends to zero as l becomes

infinite and ε goes to zero. Consequently, the mixed-phase region has a cusp at the origin of the σ, ε plane.

The boundary between α (or β) and the mixed phase is also the limit of stability of this phase against the creation of a defect. The defect of interest is that shown in Fig. 1b in which a segment of phase β of length m is inserted into phase α at a cost in free energy given by (2.4), which is just the left side of (4.17). The free energy of the defect depends, of course, on m, and the limit of stability is determined by that m which minimizes the defect energy, i.e., precisely by (4.17). At all larger values of σ the phase α is stable against formation of these defects. Of course the same argument applies to phase β when ε is positive: the left side of (4.18) is the free energy required to create a defect consisting of a segment of phase α of length l inserted into phase β.

A typical phase diagram for case B, in the situation where ϕ_α is positive and ϕ_β has a unique minimum at $m = m^\circ$ (Fig. 6), is shown in Fig. 9. Inside the mixed phase region, Eqs. (4.10)–(4.16) apply just as in case A; the only difference is that m and $\bar{m}$ are always less than or equal to m°.

The boundary between α and the mixed phase region is described by (4.17), but with $m \leqslant m^\circ$, so there are only a finite number of segments. The last segment, with $m = m^\circ$, meets the first-order α–β transition at $\varepsilon = 0$ and $\sigma = \sigma_b$, with

$$\sigma_b = -\phi_\beta(m^\circ)/2 \tag{4.21}$$

The boundary between β and the mixed phase region corresponds to a lower tangent line of zero slope through the minimum of ϕ_β, and thus to

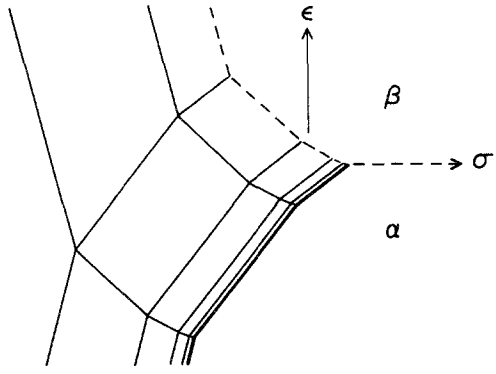

Fig. 9. Phase diagram for case B in the σ, ε plane.

$\eta_\beta = 0$, $s_\beta = -2\sigma_b$. As a consequence, $\varepsilon_\beta = f$ and $\eta_\alpha = \varepsilon$, so that on this boundary

$$2(\sigma - \sigma_b) + \phi_\alpha(l) + \varepsilon l = 0 \tag{4.22}$$

where, once again, l is the value which minimizes $\phi_\alpha(l) + \varepsilon l$ for a given ε. A comparison with (4.19) shows that the functional form of the boundary is the same as in case A, but shifted toward larger σ by an amount σ_b. Hence the point where β, $[lm^\circ]$, and $[\bar{l}m^\circ]$ come together is given by (4.20) if σ_b is added to the right side of the first equation. As l becomes infinite, the points accumulate at $\varepsilon = 0$, $\sigma = \sigma_b$.

The α-to-mixed boundary is an accumulation of superdegenerate lines, as in case A, while the β-to-mixed boundary is first order, as can be seen from the following argument. The cost in free energy of inserting into phase β a segment of $[lm^\circ]$ consisting of n pieces, each of length l, of phase α separated by $(n-1)$ pieces, each of length m°, of phase β is

$$\Delta H = 2n\sigma + n[\phi_\alpha(l) + l\varepsilon] + (n-1)\,\phi_\beta(m^\circ) = 2\sigma_b \tag{4.23}$$

where we have used (4.21) and (4.22). Consequently, the surface tension between β and $[lm^\circ]$ is σ_b, independent of l (in the pair approximation). The first-order character also follows from the fact that the boundary occurs at a value of σ, (4.22), at which the energy to create a defect, the left side of (4.19), is always positive. Hence, at this boundary β is stable against the formation of defects.

The other possibility for case B, in which ϕ_β is always positive and ϕ_α has a negative minimum at l°, can be analyzed in the same way. The phase diagram is the reflection of Fig. 9 through the σ axis. The β-to-mixed boundary is given by (4.19) with $l \leqslant l^\circ$, and the α-to-mixed boundary by

$$2(\sigma - \sigma_a) + \phi_\beta(m) - m\varepsilon = 0 \tag{4.24}$$

with m the value minimizing $\phi_\beta(m) - m\varepsilon$ for a given ε, and

$$\sigma_a = -\phi_\alpha(l^\circ)/2 \tag{4.25}$$

The coordinates of the three-phase point where α, $[l^\circ m]$, and $[l^\circ \bar{m}]$ meet are given by (4.18) if σ_a is added to the right side of the first equation. And the surface tension between α and $[l^\circ, m]$ is σ_a, independent of m. Finally, the left end of the first-order line between α and β is at $\varepsilon = 0$, $\sigma = \sigma_a$.

Case C, in which ϕ_α and ϕ_β have negative minimum at l° and m°, respectively, presents no surprise in view of the foregoing analysis. The phase diagram, Fig. 10, has first-order α-to-mixed and β-to-mixed boundaries given by (4.24) and (4.22), respectively, along which the surface

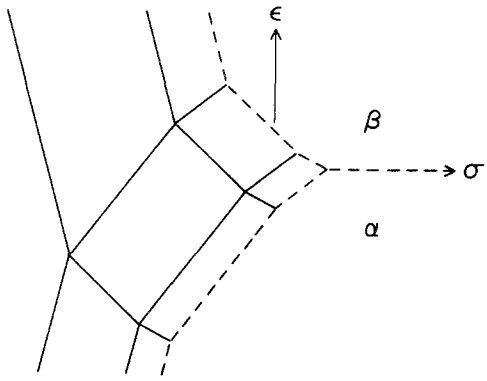

Fig. 10. Phase diagram for case C in the σ, ε plane.

tension between α and the mixed phases is equal to σ_a, (4.25), and between β and the mixed phases is σ_b, (4.21). These boundaries meet the α–β boundary at a genuine triple point located at $\varepsilon = 0$, $\sigma = \sigma_a + \sigma_b$, where the three phases α, β, and $[l^\circ m^\circ]$ coexist. The mixed-phase region contains phases which $l \leqslant l^\circ$ and $m \leqslant m^\circ$, and provided l, $\bar{l}$ and m, $\bar{m}$ do not exceed these bounds, (4.10)–(4.16) apply.

It is worth noting that in all cases the phase diagram for the mixed phase region in the σ, ε plane is the image under (4.6) and (4.14) of the corresponding diagram in the positive η_α, η_β quadrant, and the remaining first-order line separating α and β extends to the right along the σ axis from the image of $\eta_\alpha = 0$, $\eta_\beta = 0$.

5. EFFECTS OF THREE-INTERFACE INTERACTIONS

We now consider modifications of the phase diagrams of Section 4 produced by the three-interface terms $\phi_\alpha(l, m)$ and $\phi_\beta(m, l)$ in (2.10), assuming that all ϕ's with three or more arguments are zero. As mentioned earlier, we expect qualitative modifications only at superdegenerate lines and points, while first-order transitions will remain unaltered.

In fact, the only significant changes occur near points of intersection (in the pair approximation) of two superdegenerate lines. Near such a point, l_i and m_i can each take on only two possible values, which we denote by l, $\bar{l}$ and m, $\bar{m}$, with

$$\bar{l} = l + Q_\alpha, \qquad \bar{m} = m + Q_\beta \tag{5.1}$$

Thus, any configuration of interest can be represented by a string of letters,

such as $...lm\bar{l}m\bar{l}\bar{m}...$, in which l and m alternate and some letters carry bars. Our task is to find strings which minimize the "free energy" expression

$$\mathscr{H}_0 = \sum_{i=1}^{v} [l_i\eta_\alpha + m_i\eta_\beta + \phi_\alpha(l_i) + \phi_\beta(m_i) + \phi_\alpha(l_i, m_i) + \phi_\beta(m_i, l_{i+1})] \tag{5.2}$$

for a given number of letters [i.e., for fixed v: see the discussion following (2.16)]. Since l_i and m_i can only take on two values, the problem of minimizing (5.2) is completely analogous to finding the ground state of a particular one-dimensional Ising model with nearest-neighbor interactions and two atoms in a unit cell.

The configurations of interest can be thought of as walks on the energy graph shown in Fig. 11a, which functions in the present context in the same way as Fig. 4 in Section 3. The free energy $\mathscr{H}_0$ is a sum of weights associated with the vertices and edges in an obvious manner: e.g., $\bar{l}\eta_\alpha + \phi_\alpha(\bar{l})$ for the vertex $\bar{l}$, and $\phi_\beta(\bar{m}, l)$ for the edge directed from $\bar{m}$ to l. As in Section 3, the ground state graph is the subgraph of the energy graph consisting of all edges which belong to some periodic ground state: a periodic configuration which minimizes (over all periodic configurations) the free energy per letter, $\mathscr{H}_0/2v$, and thus corresponds to a cycle on the graph with the minimum possible cyclic average weight. The ground state graph depends, of course, on the parameters in $\mathscr{H}_0$. Some possibilities are shown in Fig. 11, where (b)–(d) are examples of simple cycles corresponding to the nondegenerate ground state $[\bar{l}m]$, $[l\bar{m}]$, and $[lm\bar{l}\bar{m}]$, while (e)–(h) are possible degenerate ground states. In (e), $[\bar{l}m]$ and $[l\bar{m}]$ coexist at a first-order transition, while (f)–(h) are examples of super-

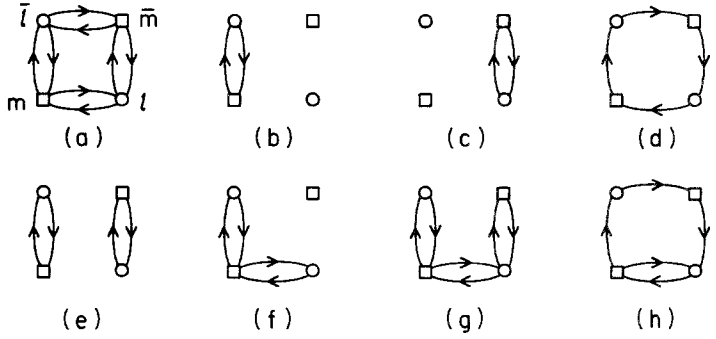

Fig. 11. (a) Energy graph and (b)–(h) various ground state graphs, assuming only configurations involving l, m, $\bar{l}$, and $\bar{m}$ are permitted.

degenerate states (see the discussion in Section 3). It is clear from the graphical analysis that first-order coexistence is possible in only two cases: $[\bar{l}m]$ with $[l\bar{m}]$ and $[\bar{l}\bar{m}]$ with $[lm]$. Otherwise, the ground state is either nondegenerate or superdegenerate. Also, there are precisely six distinct nondegenerate ground states: four two-letter states, of which Figs. 11b and 11c are examples, and two four-letter states, Fig. 11d and the one with the arrows reversed.

The qualitative nature of the phase diagram is determined by the signs of the *double differences*,

$$\Delta^2\phi_\alpha(lm) = \phi_\alpha(l, m) + \phi_\alpha(\bar{l}, \bar{m}) - \phi_\alpha(\bar{l}, m) - \phi_\alpha(l, \bar{m}) \tag{5.3}$$

$$\Delta^2\phi_\beta(ml) = \phi_\beta(m, l) + \phi_\beta(\bar{m}, \bar{l}) - \phi_\beta(\bar{m}, l) - \phi_\beta(m, \bar{l}) \tag{5.4}$$

of the three-interface interactions, as shown in the η_α, η_β plane in Fig. 12 for the cases: (a) $\Delta^2\phi_\alpha > 0$, $\Delta^2\phi_\beta > 0$; (b) $\Delta^2\phi_\alpha < 0$, $\Delta^2\phi_\beta < 0$; (c) $\Delta^2\phi_\alpha > 0$, $\Delta^2\phi_\beta < 0$; (d) $\Delta^2\phi_\alpha < 0$, $\Delta^2\phi_\beta > 0$. In each case the point where the two superdegenerate lines cross in the two-interface approximation is split apart to produce either a short first-order line, (a) and (b), or a new phase with a larger period (four letters) surrounded by a parallelogram of superdegenerate lines, (c) and (d). Away from the original intersection point, the superdegenerate lines remain parallel to the η_α and η_β axes, but the upper and lower (or left and right) segments display a small offset.

The phase diagrams in Fig. 12 are obtained by calculating $\mathscr{H}_0/v$ for each of the six nondegenerate ground states, and determining which of

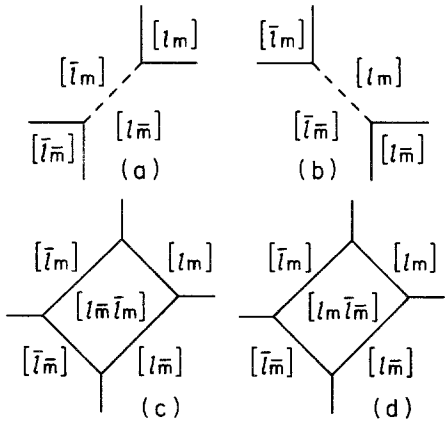

Fig. 12. Modification of the phase diagram in the η_α (horizontal), η_β (vertical) plane produced by three-interface interactions near a point where two superdegenerate lines cross in the pair approximation, Fig. 7. The cases shown are: (a) $\Delta^2\phi_\alpha > 0$, $\Delta^2\phi_\beta > 0$; (b) $\Delta^2\phi_\alpha < 0$, $\Delta^2\phi_\beta < 0$; (c) $\Delta^2\phi_\alpha > 0$, $\Delta^2\phi_\beta < 0$; (d) $\Delta^2\phi_\alpha < 0$, $\Delta^2\phi_\beta > 0$.

these has the minimum value for a given η_α and η_β. The lines separating two phases come from equating the corresponding $\mathcal{H}_0/v$ values. Appendix B gives the locations of the various three-phase points. The corresponding phase diagrams in the (σ, ε) plane can then be constructed using (4.14), and (2.17) in the form

$$-2\sigma = l\eta_\alpha + m\eta_\beta + \phi_\alpha(l) + \phi_\beta(m) + \phi_\alpha(l, m) + \phi_\beta(m, l) \tag{5.5}$$

where l and m on the right side should be replaced by $\bar{l}$ or $\bar{m}$ where appropriate. (To find σ for the line separating $[lm]$ and $[\bar{l}m]$, one can use either (5.5) as it stands or replace l by $\bar{l}$ everywhere on the right side, as σ is continuous.) Figure 13 shows the positive η_α, η_β quadrant for a particular choice of interactions for which $\Delta^2\phi_\alpha(lm)$ and $\Delta^2\phi_\beta(ml)$ are positive for all l and m. The corresponding diagram in the σ, ε plane is Fig. 14. It is not difficult to imagine what happens in other cases: the appropriate motifs appearing in Fig. 12 are strung together using the structure of super-degenerate lines already present in the pair approximation, Figs. 7 and 8. Although these figures are drawn for case A, the diagrams for cases B and C are modified in the mixed phase region in the same way as those for case A.

Where there is a first-order phase transition, as in Fig. 12a and 12b, the corresponding surface tension can be computed by considering the free energy cost of inserting a segment of one phase in the other. Consider the coexistence of $[l\bar{m}]$ with $[\bar{l}m]$. A configuration in which a segment of one is inserted in the other corresponds to a walk making use of some edges not found in the corresponding ground state graph, Fig. 11e, and there are

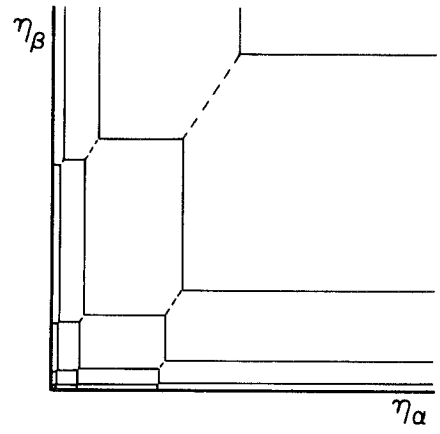

Fig. 13. Phase diagram in the positive η_α, η_β quandrant assuming $\Delta^2\phi_\alpha$ and $\Delta^2\phi_\beta$ are positive.

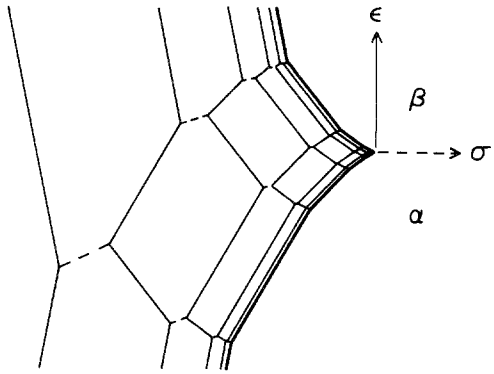

Fig. 14. Phase diagram in the σ, ε plane assuming that $\Delta^2\phi_\alpha$ and $\Delta^2\phi_\beta$ are positive.

four ways in which this can be done using only two extra edges, shown dashed in Fig. 15. A straightforward computation based on the procedures discussed in Section 2 yields the following expressions for the surface tension:

$$2\sigma_a = -(\bar{l}-l)\,\eta_\alpha + \phi_\alpha(l) - \phi_\alpha(\bar{l}) + \phi_\alpha(l, m) + \phi_\beta(m, l) - \phi_\alpha(\bar{l}, m) - \phi_\beta(m, \bar{l}) \tag{5.6}$$

$$2\sigma_b = (\bar{l}-l)\,\eta_\alpha - \phi_\alpha(l) + \phi_\alpha(\bar{l}) + \phi_\alpha(\bar{l}, \bar{m}) + \phi_\beta(\bar{m}, \bar{l}) - \phi_\alpha(l, \bar{m}) - \phi_\beta(\bar{m}, l) \tag{5.7}$$

$$2\sigma_c = \Delta^2\phi_\alpha(lm) \tag{5.8}$$

$$2\sigma_d = \Delta^2\phi_\beta(ml) \tag{5.9}$$

where the subscripts on σ correspond to the four possibilities in Fig. 15, and the expressions have been written down assuming that $\mathscr{H}_0/v$ is the same for $[l\bar{m}]$ and $[\bar{l}m]$. Note that $\sigma_a + \sigma_b$ is equal to $\sigma_c + \sigma_d$. It turns out that the minimum surface tension is σ_a near the upper right end of the first-order line in Fig. 12a, σ_b near the lower left end of this line, and near the center of the line either σ_c or σ_d is the smallest.

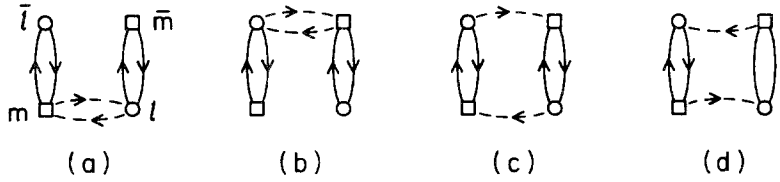

Fig. 15. Graphs illustrating different types of interface pairs which are possible when $[l\bar{m}]$ coexists with $[\bar{l}m]$. The edges used in producing the interfaces are shown in dashed lines.

6. EFFECT OF HIGHER-ORDER INTERACTIONS ON SUPERDEGENERATE LINES

The phase diagrams obtained in the three-interface approximation in Section 5 will be further modified at superdegenerate points and lines due to the effects of higher-order interactions. We begin with the lines, and consider, in particular, a superdegenerate line where $[lm]$ and $[\bar{l}m]$ come together. The configurations of interest can then be represented as strings of alternating l's and m's, with some of the l's (but none of the m's) carrying a bar. It is convenient to analyze this situation by regarding the $\bar{l}$'s as "defects" in an underlying "defect-free" $[lm]$ phase. A configuration can then be specified by a set of numbers $\{L_k\}$, where L_k is the distance (in lattice planes) between defect k and defect $k+1$. It is clear that each L_k must be of the form

$$L = L^* + PQ \tag{6.1}$$

where the quantities

$$L^* = \bar{l} + m, \qquad Q = l + m \tag{6.2}$$

play the same role as l^* and Q_α in (2.1), and $P \geqslant 0$ is some integer. The total number of planes N is the sum of the L's.

For a configuration containing N planes, we define the *defect energy* to be

$$H_D = H - Nf_0 \tag{6.3}$$

where f_0 is the free energy per plane of $[lm]$. We then suppose, following Fisher and Szpilka[17] (though not exactly the same notation), that

$$H_D = \sum_k [E_D + W_2(L_k) + W_3(L_k, L_{k+1}) + \cdots] \tag{6.4}$$

where E_D is the (free) energy to create a defect, and W_2, W_3, etc., are interaction energies for pairs of defects, triples, etc.

To obtain E_D, imagine that a single l in $[lm]$ is changed to $\bar{l}$. Then the number of planes changes by $\Delta N = \bar{l} - l$, and the free energy by

$$\begin{aligned} \Delta H = (\bar{l} - l)\,\varepsilon_\alpha + \phi_\alpha(\bar{l}) - \phi_\alpha(l) + \phi_\beta(m, \bar{l}) - \phi_\beta(m, l) \\ + \phi_\alpha(\bar{l}, m) - \phi_\alpha(l, m) + \cdots \end{aligned} \tag{6.5}$$

Consequently, in view of (6.3),

$$E_D = \Delta H_D = \Delta H - (\bar{l} - l)\, f_0 \tag{6.6}$$

where

$$(l+m)f_0 = 2\sigma + l\varepsilon_\alpha + m\varepsilon_\beta + \phi_\alpha(l) + \phi_\beta(m) + \cdots \tag{6.7}$$

Reconnection formulas of the sort discussed in conjunction with (2.7) and (2.8) may be used to express the W's in the form

$$W = H^{(a)} + H^{(b)} - H^{(c)} - H^{(d)} \tag{6.8}$$

for appropriately chosen configurations (a), (b), (c), and (d). For $W_2(L^*)$, the appropriate choice is shown in Fig. 16, and the right side of (6.8) can be evaluated in the following way. In any vertical column in this figure which is one letter wide, the same letters occur in (a) and (b) as in (c) and (d). Thus, the ε_α and ε_β terms in (2.9), as well as the ϕ's with a single argument (pair interactions), cancel out in the difference (6.8). The same observation holds for any vertical column two letters wide, and, indeed, for any column of consecutive letters which does not include those between the pair of dashed lines in Fig. 16. Consequently, under the assumption that the ϕ's become rapidly smaller as the number of interfaces increase, the dominant contribution to $W_2(L^*)$ is the double difference associated with the column between the dashed lines,

$$W_2(L^*) \simeq \Delta^2\phi(\bar{l}m\bar{l}) = \phi(lml) + \phi(\bar{l}m\bar{l}) - \phi(lm\bar{l}) - \phi(\bar{l}ml) \tag{6.9}$$

In this expression we have used the simplified notation introduced following (2.11), in which the commas separating the arguments of ϕ are omitted, and also the subscript, which in (6.9) could be α. The general definition of a double difference $\Delta^2\phi(S)$, where S is a string of letters, some of which carry bars, is as follows. Let c and d stand for the first and last letters of S, including the bars if present. Let c' be the corresponding letter without a bar if c carries a bar, or with a bar if c does not have a bar. Thus, if $c = l$, then $c' = \bar{l}$; if $c = \bar{m}$, then $c' = m$. Define d' in the same way. Then writing S in the form cTd, we define

$$\Delta^2\phi(cTd) = \phi(cTd) + \phi(c'Td') - \phi(c'Td) - \phi(cTd') \tag{6.10}$$

Note that (5.3) and (5.4), as well as (6.9), are consistent with this notation.

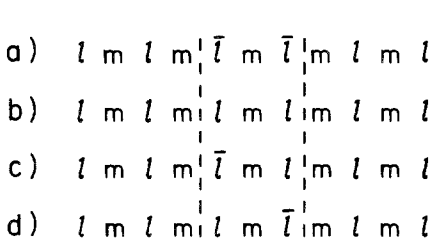

Fig. 16. Figure illustrating the reconnection formula (6.8) for $W_2(L^*)$.

The same reconnection argument can be used for the other W's. For example, one finds

$$W_3(L^*, L^* + Q) \cong \Delta^2\phi(\bar{l}m\bar{l}m\bar{l}m\bar{l}) \tag{6.11}$$

and in general the dominant contributions to $W_{n+1}(L_1, L_2, ..., L_n)$ are of the form $\Delta^2\phi(S)$, where the string S is obtained from a configuration containing $n+1$ $\bar{l}$'s (defects) separated by distances specified by $L_1, L_2, ..., L_n$. (If this approximation is not sufficient, one can write down an exact expression for W as an infinite sum; see Appendix C.)

Once the W's are known, the phase diagram can be computed following the procedure of Fisher and Szpilka: first take into account pair interactions W_2 while ignoring W_3, W_4, etc., and then see how the resulting phase diagram is modified by higher-order terms. The analysis for pair interactions is basically the same as in Section 4 above. One considers lower tangent lines to the graph of $W_2(L)$, with L taking the values allowed by (6.1). If, for example, W_2 satisfies the convexity condition

$$W_2(L+Q) + W_2(L-Q) - 2W_2(L) > 0 \tag{6.12}$$

for all $L > L^*$, the result, in the defect pair approximation, is an infinite set of periodic phases

$$[\bar{l}m], [\bar{l}m\bar{l}m], [\bar{l}m\bar{l}m\bar{l}m], ...$$

separated by superdegenerate lines. If, on the other hand, W_2 has a unique negative minimum at $L = L^\circ$, there is a first-order transition between this phase and $[lm]$. In particular, if the minimum occurs at $L^\circ = L^*$, as one would expect if (6.9) were negative, the transition from $[lm]$ to $[\bar{l}m]$ is first order, so that the higher-order interactions have transformed the original supergenerate line into a first-order transition.

If in the approximation which uses only W_2 a certain number of superdegenerate transitions remain, the effects of the remaining interactions can be evaluated using the following "renormalization" approach. Suppose a superdegenerate transition separates phases corresponding to L and $\bar{L} = L + Q$. Then the configurations of interest will be of the form $L\bar{L}\bar{L}L...$, etc., where L and $\bar{L}$ are associated with appropriate sequences of l's, $\bar{l}$'s, and m's. We may consider $[L] = ...LLL...$ as a reference state, and the $\bar{L}$'s as constituting a new kind of defect. The distances $\{\tilde{L}_k\}$ between the new defects are of the form

$$\tilde{L} = \tilde{L}^* + \tilde{P}\tilde{Q} \tag{6.13}$$

where

$$\tilde{L}^* = \bar{L}, \qquad \tilde{Q} = L \tag{6.14}$$

and $\tilde{P}$ is any nonnegative integer. In analogy with (6.3) and (6.4), we introduce

$$\tilde{H}_D = H - Nf_L \tag{6.15}$$

where f_L is the free energy per plane for the phase $[L]$, and write

$$\tilde{H}_D = \sum_k [\tilde{E}_D + \tilde{W}_2(\tilde{L}_k) + \tilde{W}_3(\tilde{L}_k, \tilde{L}_{k+1}) + \cdots] \tag{6.16}$$

The $\tilde{W}$'s and $\tilde{E}_D$ can be computed directly in terms of the quantities in (2.9), or expressed in terms of the W's and E_D. Formulas of the latter type are given in Appendix D.

Of course one cannot make definite statements about the ultimate phase diagram resulting from taking all the interactions into account without having some reasonably explicit functional form for the ϕ's. We shall discuss one such from in Section 8 below. The methods of this section also apply at a superdegenerate line separating $[lm]$ and $[l\bar{m}]$, with an obvious change in notation. But in addition, the same strategy works in more complex cases, such as the line separating $[lm]$ and $[lm\bar{l}\bar{m}]$ in Fig. 12d. One must, however, remember that the analysis is only valid when the configurations which need to be taken into account are precisely those which are allowed on the original superdegenerate line. This is no longer the case near a point where one superdegenerate line meets another. We consider one such point in the next section.

7. EFFECT OF HIGHER-ORDER INTERACTIONS AT A SUPERDEGENERATE POINT

The points at the ends of the first-order (dashed) lines in Figs. 12a and 12b bear a certain resemblance to Fig. 5, the phase diagram obtained by ignoring interface interactions. This observation provides the key to analyzing the effects of higher-order interactions on the phase diagram near one of these points.

To be specific, we shall analyze the point in Fig. 12a where the phases $[lm]$, $[l\bar{m}]$, and $[\bar{l}m]$ come together. The corresponding ground state graph in the three-interface approximation of Section 5 is the one shown in Fig. 11g, and we shall assume that only configurations corresponding to walks on this graph need be considered. Such configurations can be represented in an obvious way as strings of alternating m's and l's, with bars on some of the letters. However, no two letters adjacent to one another can both carry a bar. Consequently, any allowed configuration can be regarded as an admixture of the two phases

$$\tilde{\alpha} = [\bar{l}m], \qquad \tilde{\beta} = [l\bar{m}] \tag{7.1}$$

associated with the left and right vertical loops of Fig. 11g, with an interface arising whenever the walk utilizes one of the horizontal edges in this figure, that is, whenever a letter without a bar is followed by another letter with no bar.

Thus, the possible lengths $\tilde{l}$ and $\tilde{m}$ (in planes, not letters) of segments of phases $\tilde{\alpha}$ and $\tilde{\beta}$ have the form

$$\tilde{l} = \tilde{l}^* + \tilde{p}\tilde{Q}_\alpha \tag{7.2}$$

$$\tilde{m} = \tilde{m}^* + \tilde{q}\tilde{Q}_\beta \tag{7.3}$$

in analogy with (2.1) and (2.2), where

$$\begin{aligned} \tilde{l}^* &= m, \qquad \tilde{Q}_\alpha = \bar{l} + m \\ \tilde{m}^* &= l, \qquad \tilde{Q}_\beta = l + \bar{m} \end{aligned} \tag{7.4}$$

and $\tilde{p}$ and $\tilde{q}$ are nonnegative integers. Note that the shortest possible segment of $\tilde{\alpha}$ consists of m successive planes of phase β, while the shortest segment of $\tilde{\beta}$ contains l planes of α. An allowed configuration is specified by the sequence $\{\tilde{l}_k, \tilde{m}_k\}$ giving the lengths of successive segments of $\tilde{\alpha}$ and $\tilde{\beta}$, and the total number of planes is

$$N = \sum_{k=1}^{\tilde{\nu}} (\tilde{l}_k + \tilde{m}_k) \tag{7.5}$$

in analogy with (2.11), where $2\tilde{\nu}$ is the number of interfaces between $\tilde{\alpha}$ and $\tilde{\beta}$.

The free energy (2.9) of an allowed configuration can be written in the form

$$\tilde{H} = \sum_k (2\tilde{\sigma} + \tilde{l}_k \tilde{\varepsilon}_\alpha + \tilde{m}_k \tilde{\varepsilon}_\beta) + \tilde{\Phi} \tag{7.6}$$

with

$$\tilde{\Phi} = \sum_k [\tilde{\phi}_\alpha(\tilde{l}_k) + \tilde{\phi}_\beta(\tilde{m}_k) + \tilde{\phi}_\alpha(\tilde{l}_k, \tilde{m}_k) + \cdots] \tag{7.7}$$

the analogy of (2.10). But note that while $\tilde{H} = H$, $\tilde{\Phi}$ is not equal to Φ! In analogy with (2.13), we define

$$\tilde{\varepsilon} = \tilde{\varepsilon}_\alpha - \tilde{\varepsilon}_\beta \tag{7.8}$$

By equating $\tilde{H}$ and H, the various quantities in (7.6) and (7.7) can be

related to those in (2.9) and (2.10). Thus, $\tilde{\varepsilon}_\alpha$ and $\hat{\varepsilon}_\beta$ are the free energies per plane of the "pure" phases $\tilde{\alpha}$ and $\tilde{\beta}$, and hence given by the formulas

$$(\bar{l}+m)\,\tilde{\varepsilon}_\alpha = 2\sigma + \bar{l}\varepsilon_\alpha + m\varepsilon_\beta + \psi_\alpha \tag{7.9}$$

$$(l+\bar{m})\,\tilde{\varepsilon}_\beta = 2\sigma + l\varepsilon_\alpha + \bar{m}\varepsilon_\beta + \psi_\beta \tag{7.10}$$

where

$$\psi_\alpha = \phi_\alpha(\bar{l}) + \phi_\beta(m) + \phi_\alpha(\bar{l}, m) + \phi_\beta(m, \bar{l}) + \cdots \tag{7.11}$$

is the contribution of Φ to the free energy of $\bar{l}+m$ planes of phase $\tilde{\alpha}$, and

$$\psi_\beta = \phi_\alpha(l) + \phi_\beta(\bar{m}) + \phi_\alpha(l, \bar{m}) + \phi_\beta(\bar{m}, l) + \cdots \tag{7.12}$$

is its counterpart for phase $\tilde{\beta}$. Taking the difference yields

$$\tilde{\varepsilon} = \frac{2(l-\bar{l}-m+\bar{m})\sigma + (\bar{l}\bar{m} - lm)\varepsilon}{(l+\bar{m})(\bar{l}+m)} + \frac{\psi_\alpha}{\bar{l}+m} - \frac{\psi_\beta}{l+\bar{m}} \tag{7.13}$$

The $\tilde{\phi}$'s can be evaluated using reconnection formulas as discussed in Section 2, in connection with (2.7) and (2.8), and employed in Section 6 to obtain the "defect" interactions. The standard form is

$$\tilde{\phi} = H^{(a)} + H^{(b)} - H^{(c)} - H^{(d)} \tag{7.14}$$

for appropriately chosen configurations (a), (b), (c), and (d). The choice for $\tilde{\phi}_\beta(\tilde{m}^*)$ is shown in Fig. 17, where a thin underline indicates $\tilde{\alpha}$, a heavy underline $\tilde{\beta}$, and colons have been inserted at the interfaces. The analysis is then parallel to that used in connection with (6.8) and Fig. 16. In any vertical column one or two letters wide in Fig. 17 the same letters or pairs of letters occur in (c) and (d) as in (a) and (b), so the corresponding terms—ε_α, ε_β, ϕ's involving two or three interfaces—cancel out in the dif-

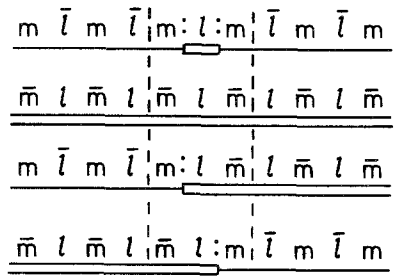

Fig. 17. Figure illustrating the reconnective formula (7.14) for $\tilde{\phi}_\beta(\tilde{m}^*)$.

ference (7.14). Indeed, only columns of consecutive letters which include those between the dashed lines make a nonzero contribution, from which it follows that the dominant contribution is

$$\tilde{\phi}_\beta(\tilde{m}^*) \cong \Delta^2\phi(mlm) \tag{7.15}$$

using the notation introduced in (6.10).

This result is easily generalized to larger values of $\tilde{m}$, or to $\tilde{\phi}_\beta$ or $\tilde{\phi}_\alpha$ with several arguments, with the following result. Any $\tilde{\phi}$ with a specific set of arguments corresponds to a set of segments of $\tilde{\alpha}$ and $\tilde{\beta}$ separated by interfaces. Let S be the string of letters consisting of l's and m's, with or without bars, extending from the first to the last of these interfaces, and in addition including the letter which precedes the first interface and the letter following the last interface, in the configuration which contains precisely this set of interfaces and no others. Then, to lowest order,

$$\tilde{\phi} \cong \Delta^2\phi(S) \tag{7.16}$$

For example, in the case of $\tilde{\phi}_\beta(\tilde{m}^*)$, S is mlm; for $\tilde{\phi}_\beta(\tilde{m}^* + \tilde{Q}_\beta)$, S is $ml\bar{m}lm$; for $\tilde{\phi}_\alpha(\tilde{l}^*, \tilde{m}^*)$, S is $lmlm$. In place of the approximation (7.16), $\tilde{\phi}$ can be expressed as an infinite sum: see Appendix C.

The term $\tilde{\sigma}$ in (7.6) can be obtained in the manner suggested by Fig. 1b and Eq. (2.4), by inserting a segment of $\tilde{\beta}$ into a pure $\tilde{\alpha}$ phase. The shortest such segment, of length $\tilde{m}^* = l$, is produced by removing a bar from a single $\bar{l}$ in an $\tilde{\alpha}$ configuration, with a resulting free energy change of

$$\begin{aligned}\Delta H = (l-\bar{l})\,\varepsilon_\alpha + \phi_\alpha(l) - \phi_\alpha(\bar{l}) \\ + \phi_\beta(m, l) - \phi_\beta(m, \bar{l}) + \phi_\alpha(l, m) - \phi_\alpha(\bar{l}, m) + \cdots\end{aligned} \tag{7.17}$$

which [see (7.6) and (7.7)] is equal to

$$\Delta\tilde{H} = 2\tilde{\sigma} + l\tilde{\varepsilon}_\beta - \bar{l}\tilde{\varepsilon}_\alpha + \tilde{\phi}_\beta(\tilde{m}^*) \tag{7.18}$$

the counterpart of (2.4). As $\tilde{\varepsilon}_\alpha$, $\tilde{\varepsilon}_\beta$, and $\tilde{\phi}_\beta(\tilde{m}^*)$ have been computed previously, equating (7.17) and (7.18) yields the expression

$$\begin{aligned}2\tilde{\sigma} = \frac{2(\bar{l}\bar{m} - lm)\sigma + [l\bar{l}(\bar{m}-m) - m\bar{m}(\bar{l}-l)]\varepsilon}{(\bar{l}+m)(l+\bar{m})} \\ + \frac{\bar{l}}{\bar{l}+m}\psi_\alpha + \frac{\bar{m}}{\bar{m}+l}\psi_\beta + \Delta_\sigma\end{aligned} \tag{7.19}$$

where ψ_α and ψ_β are defined in (7.11) and (7.12), and

$$\begin{aligned}\Delta_\sigma = -\phi_\alpha(\bar{l}) - \phi_\beta(\bar{m}) + \phi_\alpha(l, m) + \phi_\beta(m, l) \\ - \phi_\alpha(l, \bar{m}) - \phi_\beta(\bar{m}, l) - \phi_\alpha(\bar{l}, m) - \phi_\beta(m, \bar{l}) + \cdots\end{aligned} \tag{7.20}$$

See Appendix C for the general expression. One can show that $\tilde{\sigma}$ is the same as σ_a in (5.6) up to three-interface terms provided ε and σ in (7.19) are chosen so that the phases $\tilde{\alpha}$ and $\tilde{\beta}$ coexist. Note that (5.6) defines a surface tension only on the coexistence line, whereas (7.19) does not have this restriction.

The analysis of the phase diagram near the $[lm] : [l\bar{m}] : [\bar{l}m]$ point in Fig. 12a can now proceed using the methods of Sections 4 and 5, with the interactions $\tilde{\phi}$ for the new interfaces replacing ϕ. The $\tilde{\phi}$'s with a single argument, the new pair interactions, can lead to a splitting of the superdegenerate lines to produce periodic phases which can be regarded as mixtures of $\tilde{\alpha}$ and $\tilde{\beta}$, such as $[lm\bar{l}m]$, $[lml\bar{m}l\bar{m}]$, etc. Of course, not all of these phases need occur. Those which arise will be determined by the convexity (or lack thereof) of the functions $\tilde{\phi}_\alpha(\bar{l})$ and $\tilde{\phi}_\beta(\tilde{m})$, in accordance with the geometrical arguments of Section 4. If new superdegenerate lines arise, the splitups of the four-phase points where they cross will be determined by the double differences of the $\tilde{\phi}$'s with two arguments, as in Section 5.

Once any feature in the phase diagram has been located in the $\tilde{\sigma}$, $\tilde{\varepsilon}$ plane, it can be mapped back to the σ, ε plane by solving (7.13) and (7.19) for σ and ε in terms of $\tilde{\sigma}$ and $\tilde{\varepsilon}$. Note that these equations are linear in σ and ε, with coefficients which depend on l and m, that is to say, on the particular three-phase point which is being studied.

Precisely the same analysis can be carried out at the other points in Figs. 12a and 12b where a first-order line meets two superdegenerate lines. It is, of course, tedious to rederive the formulas for the different cases, so we list in Table I a set of equivalences which allows one to transform those for the case discussed above, corresponding to the first line of the table, to the corresponding formulas for the other cases. Line 1 of the table corresponds to the case we have discussed, with $\tilde{\gamma}$ the phase between the superdegenerate lines in Fig. 12. If one is, for example, interested in the point where $[\bar{l}\bar{m}]$, $[lm]$, and $[\bar{l}m]$ come together, in Fig. 12b, then line 2 of the table shows which phase should be identified as $\tilde{\alpha}$ and which as $\tilde{\beta}$.

Table I. Equivalences for Transforming Formulas for Renormalized Quantities

	$\tilde{\alpha}$	$\tilde{\beta}$	$\tilde{\gamma}$							
1.	$[\bar{l}m]$	$[l\bar{m}]$	$[lm]$	l	$\bar{l}$	m	$\bar{m}$	ε_α	ε_β	ε
2.	$[\bar{l}\bar{m}]$	$[lm]$	$[\bar{l}m]$	m	$\bar{m}$	$\bar{l}$	l	ε_β	ε_α	$-\varepsilon$
3.	$[l\bar{m}]$	$[lm]$	$[\bar{l}\bar{m}]$	$\bar{l}$	l	$\bar{m}$	m	ε_α	ε_β	ε
4.	$[lm]$	$[\bar{l}\bar{m}]$	$[l\bar{m}]$	$\bar{m}$	m	l	$\bar{l}$	ε_β	ε_α	$-\varepsilon$

Then equations (7.4), (7.9), (7.10), (7.13), and (7.19) remain valid provided the quantities carrying tildes are left unchanged, while each l is replaced by m, $\bar{l}$ by $\bar{m}$, m by $\bar{l}$, and $\bar{m}$ by l, and the same replacement is carried out in (7.11), (7.12), and (7.20), the formulas for ϕ_α, ψ_β, and Δ_σ. In addition, the subscripts on the ϕ's must be altered appropriately; thus, for example, $\phi_\alpha(\bar{l}, m)$ in (7.11) is replaced by $\phi_\beta(\bar{m}, \bar{l})$. Finally, ε_α becomes ε_β and vice versa, and hence ε is to be replaced by $-\varepsilon$. The same substitution rule works for the $\tilde{\phi}$'s. Thus, $\tilde{\phi}_\beta(\tilde{m}^*)$ is $\Delta^2\phi(\bar{l}m\bar{l})$ to lowest order, and $\tilde{\phi}_\alpha(\tilde{l}^*, \tilde{m}^*)$ is $\Delta^2\phi(m\bar{l}m\bar{l})$ which, note, is $-\Delta^2\phi(m\bar{l}ml)$ according to the definition adopted in Section 6.

8. PHASE DIAGRAMS FOR EXPONENTIAL INTERACTIONS

Sasaki[18] has shown that in the case of a Frenkel–Kontorova model, under fairly general assumptions, the interface interactions ϕ_α and ϕ_β have the following form if the interactions are sufficiently far apart. In the case of pairs of interfaces,

$$\phi_\alpha(l) = C_\alpha \Lambda_\alpha^p, \qquad \phi_\beta(m) = C_\beta \Lambda_\beta^q \tag{8.1}$$

where p and q are related to l and m through (2.1) and (2.2), and C_α, Λ_α, C_β, and Λ_β are real constants, with of course

$$|\Lambda_\alpha| < 1, \qquad |\Lambda_\beta| < 1 \tag{8.2}$$

Higher-order interactions are given by a factorization rule:

$$\begin{aligned} \phi_\alpha(l, m) &= \phi_\alpha(l)\, \phi_\beta(m)\, t_{\alpha\beta} \\ \phi_\beta(m, l) &= \phi_\beta(m)\, \phi_\alpha(l)\, t_{\beta\alpha} \end{aligned} \tag{8.3}$$

and, in general,

$$\begin{aligned} \phi_\alpha(l_1, m_1, l_2, \ldots) &= \phi_\alpha(l_1)\, \phi_\beta(m_1)\, \phi_\alpha(l_2) \cdots t_{\alpha\beta} t_{\beta\alpha} \cdots \\ \phi_\beta(m_1, l_2, m_2, \ldots) &= \phi_\beta(m_1)\, \phi_\alpha(l_2)\, \phi_\beta(m_2) \cdots t_{\beta\alpha} t_{\alpha\beta} \cdots \end{aligned} \tag{8.4}$$

where a factor of $t_{\alpha\beta}$ appears for every pair of successive arguments in which an m follows an l, and $t_{\beta\alpha}$ when an l follows an m. Thus, there is one less t than there are arguments of ϕ. Alternatively, one can say that there is a $t_{\alpha\beta}$ for every α-to-β and a $t_{\beta\alpha}$ in every β-to-α interface whose interaction is represented by ϕ, except for the first and the last interface.

In the case of a Frenkel–Kontorova model these formulas are only approximate; they become asymptotically exact (with exponentially small corrections) as the p's and q's become large. One can, of course, simply

regard (8.1)–(8.4) as defining a "model" set of interactions which shall, for brevity, be referred to as *exponential interactions.*

The set of exponential interactions is determined by six real parameters: C_α, C_β, Λ_α, Λ_β, $t_{\alpha\beta}$, $t_{\beta\alpha}$. However, the qualitative features of the phase diagram are determined by the *signs* of these quantities. In particular, the convexity condition (4.8) for ϕ_α is satisfied for all $l > l^*$ if and only if C_α and Λ_α are both positive. If C_α is negative, ϕ_α has a unique negative minimum at $l^\circ = l^*$, and if C_α is positive but Λ_α is negative, the unique negative minimum is at $l^\circ = l^* + Q_\alpha$. Analogous comments apply to ϕ_β, C_β, and Λ_β. Therefore, case A of Section 4 arises when C_α, Λ_α, C_β, and Λ_β are all positive, case B when either C_α and Λ_α are positive, or C_β and Λ_β are positive, but not all four are positive, and case C in all other instances.

Let us restrict our attention to what happens in the immediate vicinity of the point U on the phase diagram where the first-order line separating phases α and β comes to an end and the multiphase region begins. Case C is then relatively uninteresting, as already in the pair interaction approximation U is a triple point with a first-order coexistence of three phases, Fig. 10, and this situation will not be altered by (weak) higher-order interactions.

Case B is more interesting, since in the pair approximation, Fig. 9, U is an accumulation point of "superdegenerate endpoints" where superdegenerate lines meet the first-order β-to-mixed transition, assuming that C_α and Λ_α are positive. The effect of higher-order interactions on one of these superdegenerate lines can then be worked out by the method discussed in Section 6, setting $m = m^\circ$ (the minimum of ϕ_β) in the formulas for W. One can show that in this case W has the "exponential" form

$$W_{n+1}(L_1, L_2, \ldots, L_n) = D\mu^{n-1}\Lambda^{P_1 + P_2 + \cdots + P_n} \tag{8.5}$$

where P_j is related to L_j through (6.1), and

$$\Lambda = C_\alpha \Lambda_\alpha^p C_\beta \Lambda_\beta^q t_{\alpha\beta} t_{\beta\alpha} \tag{8.6}$$

$$\mu = \Lambda_\alpha \Lambda \tag{8.7}$$

$$D = C_\alpha \Lambda_\alpha^p \Lambda \tag{8.8}$$

to lowest order. Note that p can be any nonnegative integer, but q is either 0 or 1, depending on whether $m^\circ = m^*$ or $m^\circ = m^* + Q_\beta$; the latter occurs in the case $C_\beta > 0$, $\Lambda_\beta < 0$.

There are now two distinct possibilities, depending on the sign of

$$C_\beta \Lambda_\beta^q t_{\alpha\beta} t_{\beta\alpha} \tag{8.9}$$

If this quantity is negative, then Λ and D are negative, and we need only consider the pair approximation $W_2(L)$ to see that the superdegenerate line becomes a first-order transition. As this happens for every superdegenerate line, whatever the value of p, we conclude that the α-to-mixed boundary becomes a *quasicontinuous* transition, by which we mean an accumulation of an infinite number of first-order transitions which become smaller and smaller upon approaching the α phase (what Fisher and Szpilka[17] call a "devil's last step"). Consequently, U is a quasicontinuous endpoint: the point where the phenomenon just described terminates on a first-order line.

The other possibility is that (8.9) is positive. In that case D, Λ, and μ are all positive, and W_2 satisfies the convexity condition (6.12), so that the superdegenerate line in question is split into an infinity of superdegenerate lines in the defect pair approximation (using W_2). At one of these lines, characterized by L corresponding to P and $\bar{L}$ to $P+1$, it is possible to compute the renormalized interactions in (6.16). These turn out to have the same exponential form (8.5) with a new set of parameters, obtained using the formulas of Appendix D:

$$\tilde{D} = D\mu\Lambda^{2P} \tag{8.10}$$

$$\tilde{\Lambda} = \mu\Lambda^{P} \tag{8.11}$$

$$\tilde{\mu} = \mu\Lambda^{P+1} \tag{8.12}$$

to lowest order. But since D, Λ, and μ are positive, the same is true of $\tilde{D}$, $\tilde{\Lambda}$, and $\tilde{\mu}$. Furthermore, this property will hold for all subsequent renormalizations. Hence, we conclude that as higher and higher-order interactions are considered, the superdegenerate lines will continue to subdivide on a finer and finer scale, resulting in a *singular continuous* transition in which phases of arbitrarily large periodicity appear in the phase diagram, together with nonperiodic phases obtained as limits. Such a structure is commonly called a "devil's staircase," and is typical of a "commensurate–incommensurate" transition. In this case U is the endpoint where the boundary of this singular-continuous (or devil's staircase, etc.) structure at the α phase meets a first-order transition.

In case A, C_α, Λ_α, C_β, and Λ_β are all positive, but $t_{\alpha\beta}$ and $t_{\beta\alpha}$ can be of either sign. We begin by analyzing the effects of higher-order interactions on the superdegenerate lines, Fig. 8, which arise in the pair approximation. Away from the four-phase points where they intersect, the analysis in Section 6 can be used, and formulas (8.5)–(8.8), together with their counterparts when α and β are interchanged, are applicable. It follows from the preceding discussion of case B that the superdegenerate lines either become first order, if $t_{\alpha\beta}t_{\beta\alpha}$ is negative, or broaden into singular-continuous (devil's staircase) transitions if $t_{\alpha\beta}t_{\beta\alpha}$ is positive.

Near the four-phase points of the pair approximation, the analysis of Section 5 can be applied. Inserting (8.3) into (5.3) and (5.4) yields the formulas

$$\Delta^2\phi_\alpha(lm) = t_{\alpha\beta}[\phi_\alpha(l) - \phi_\alpha(\bar{l})][\phi_\beta(m) - \phi_\beta(\bar{m})] \tag{8.13}$$

$$\Delta^2\phi_\beta(ml) = t_{\beta\alpha}[\phi_\alpha(l) - \phi_\alpha(\bar{l})][\phi_\beta(m) - \phi_\beta(\bar{m})] \tag{8.14}$$

Since $\bar{l}$ is larger than l and $\bar{m}$ larger than m, (5.1), $\Delta^2\phi_\alpha$ has the same sign as $t_{\alpha\beta}$, and $\Delta^2\phi_\beta$ the sign of $t_{\beta\alpha}$. Consequently, the four cases shown in Fig. 12 correspond to: (a) $t_{\alpha\beta} > 0$, $t_{\beta\alpha} > 0$; (b) $t_{\alpha\beta} < 0$, $t_{\beta\alpha} < 0$; (c) $t_{\alpha\beta} > 0$, $t_{\beta\alpha} < 0$; (d) $t_{\alpha\beta} < 0$, $t_{\beta\alpha} > 0$.

When $t_{\alpha\beta}t_{\beta\alpha}$ is negative, one can show that higher-order interactions transform the superdegenerate lines surrounding the inner parallelograms in Figs. 12c and 12d into first-order transitions, which therefore join the first-order lines parallel to the η_α and η_β axes at ordinary triple points. Consequently, the mixed-phase region is filled with a fairly complicated array of first-order lines and triple points, and the point U is a "quasi-continuous" accumulation point of an infinite set of such transitions.

When $t_{\alpha\beta}t_{\beta\alpha}$ is positive, the analysis of Section 7 can be applied to the three-phase points in Figs. 12a and 12b. First consider the case (a), $t_{\alpha\beta} > 0$, $t_{\beta\alpha} > 0$, and in particular the point where $[\bar{l}m]$, $[l\bar{m}]$, and $[lm]$ come together. The approximation (7.16) applied to the exponential interactions (8.1)–(8.4) yields renormalized interactions $\tilde{\phi}$ with the same functional form, but a new set of constants given by the formulas

$$\tilde{\Lambda}_\alpha = C_\alpha \Lambda_\alpha^{\bar{p}} C_\beta \Lambda_\beta^{q} t_{\alpha\beta} t_{\beta\alpha} \tag{8.15}$$

$$\tilde{\Lambda}_\beta = C_\alpha \Lambda_\alpha^{p} C_\beta \Lambda_\beta^{\bar{q}} t_{\alpha\beta} t_{\beta\alpha} \tag{8.16}$$

$$\tilde{C}_\alpha = [C_\alpha(\Lambda_\alpha^{p} - \Lambda_\alpha^{\bar{p}})]^2 C_\beta \Lambda_\beta^{q} t_{\alpha\beta} t_{\beta\alpha} \tag{8.17}$$

$$\tilde{C}_\beta = C_\alpha \Lambda_\alpha^{p} [C_\beta(\Lambda_\beta^{q} - \Lambda_\beta^{\bar{q}})]^2 t_{\alpha\beta} t_{\beta\alpha} \tag{8.18}$$

$$\tilde{t}_{\alpha\beta} = [t_{\beta\alpha} C_\alpha(\Lambda_\alpha^{p} - \Lambda_\alpha^{\bar{p}})\, C_\beta(\Lambda_\beta^{q} - \Lambda_\beta^{\bar{q}})]^{-1} \tag{8.19}$$

$$\tilde{t}_{\beta\alpha} = [t_{\alpha\beta} C_\alpha(\Lambda_\alpha^{p} - \Lambda_\alpha^{\bar{p}})\, C_\beta(\Lambda_\beta^{q} - \Lambda_\beta^{\bar{q}})]^{-1} \tag{8.20}$$

where p and $\bar{p}$ are associated with l and $\bar{l}$, respectively, through (2.1), and q and $\bar{q}$ with m and $\bar{m}$ through (2.2). Replacing p by $\bar{p}$, $\bar{p}$ by p, q by $\bar{q}$, and $\bar{q}$ by q on the right side of each of these formulas makes them applicable at the other three-phase point in Fig. 12a, where $[l\bar{m}]$, $[\bar{l}m]$, and $[\bar{l}\bar{m}]$ come together.

As the C's, Λ's, and t's are all positive, and since $\bar{p}$ is greater than p and $\bar{q}$ greater than q, formulas (8.15)–(8.20) tell us that the $\tilde{C}$'s, $\tilde{\Lambda}$'s, and $\tilde{t}$'s are also positive. This same property will obviously be preserved under

further renormalizations. Consequently, each of the three-phase points in Fig. 14 will, under the effects of further perturbations, turn into a microscopic version of U, with a complex set of singular-continuous transitions, but also another infinite set of (much smaller) first-order lines in its vicinity, and with each end of each of these lines there is associated a similar structure, and so on ad infinitum. Thus, the phase diagram has a self-similar or "fractal" stucture. In this case we shall refer to U as an *upsilon point*, since the first-order line and outer boundaries of the mixed-phase region, Fig. 14, resemble the letter Υ lying on its side. Evidently, an upsilon point is a point of accumulation of (other) upsilon points.

Finally, consider the case $t_{\alpha\beta} < 0$, $t_{\beta\alpha} < 0$, and in particular the point where $[\bar{l}\bar{m}]$, $[lm]$, and $[\bar{l}m]$ come together in Fig. 12b. Making appropriate substitutions, as indicated in line 2 of Table I, in the formulas of Section 7 yields a set of renormalized interactions $\tilde{\phi}$ described by the constants given by the formulas

$$\tilde{\Lambda}_\alpha = C_\alpha \Lambda_\alpha^{\bar{p}} C_\beta \Lambda_\beta^{\bar{q}} t_{\alpha\beta} t_{\beta\alpha} \tag{8.21}$$

$$\tilde{\Lambda}_\beta = C_\alpha \Lambda_\alpha^{p} C_\beta \Lambda_\beta^{q} t_{\alpha\beta} t_{\beta\alpha} \tag{8.22}$$

$$\tilde{C}_\alpha = C_\alpha \Lambda_\alpha^{\bar{p}} [C_\beta (\Lambda_\beta^{q} - \Lambda_\beta^{\bar{q}})]^2 \, t_{\alpha\beta} t_{\beta\alpha} \tag{8.23}$$

$$\tilde{C}_\beta = [C_\alpha (\Lambda_\alpha^{p} - \Lambda_\alpha^{\bar{p}})]^2 \, C_\beta \Lambda_\beta^{q} t_{\alpha\beta} t_{\beta\alpha} \tag{8.24}$$

$$\tilde{t}_{\alpha\beta} = -[t_{\alpha\beta} C_\alpha (\Lambda_\alpha^{p} - \Lambda_\alpha^{\bar{p}}) \, C_\beta (\Lambda_\beta^{q} - \Lambda_\beta^{\bar{q}})]^{-1} \tag{8.25}$$

$$\tilde{t}_{\beta\alpha} = -[t_{\beta\alpha} C_\alpha (\Lambda_\alpha^{p} - \Lambda_\alpha^{\bar{p}}) \, C_\beta (\Lambda_\beta^{q} - \Lambda_\beta^{p} - \Lambda_\beta^{\bar{q}})]^{-1} \tag{8.26}$$

with the same association of p with l, $\bar{p}$ with $\bar{l}$, q with m, and q with $\bar{m}$ noted earlier. Replacing p with $\bar{p}$, $\bar{p}$ with p, q with $\bar{q}$, and $\bar{q}$ with q in these formulas makes them applicable at the three-phase point $[lm]$, $[\bar{l}\bar{m}]$, and $[l\bar{m}]$ in Fig. 12b.

While (8.21)–(8.26) resemble (8.15)–(8.20), one crucial difference is the minus sign on the right side of (8.25) and (8.26). This means that since $t_{\alpha\beta}$ and $t_{\beta\alpha}$ are negative, $\tilde{t}_{\alpha\beta}$ and $\tilde{t}_{\beta\alpha}$ will be positive, along with the $\tilde{C}$'s and $\tilde{\Lambda}$'s. This has the following consequence for the phase diagram. In the vicinity of the point U there are an infinite number of first-order transitions which are (roughly) perpendicular to the main first-order line separating phases α and β. At each end of each of these first-order lines one finds an upsilon point as previously defined (with the t's positive): in its vicinity there will be an infinite number of first-order transitions which are (roughly) parallel to the first-order line terminating on the upsilon point, and thus again (roughly) perpendicular to the $\alpha\beta$ transition line. Perhaps U should be called an "inverse" upsilon point to distinguish it from the "normal"

upsilon point previously defined. In any case, U is an accumulation point of (normal) upsilon points.

9. CONCLUSION

We have shown that model of interacting interfaces introduced in Section 2 can be analyzed in considerable detail, using the strategy employed earlier by Fisher and Szpilka[17] for defects, assuming that the interaction decreases rapidly with the number of interfaces and with the distance between interfaces. The qualitative features of the resulting phase diagram depend in a crucial way on the convexity, or lack thereof, of the pair interactions, (4.8) and (4.9), and on the signs of certain double differences, as defined in (5.3), (5.4), and (6.10), involving higher-order interactions.

Whereas we have not attempted to work out the most general case involving arbitrary sets of interface interactions, we have shown in Sections 6 and 7 how certain cases can, at least in principle, be attacked by iterative methods using sets of defects, or "renormalized" defects, and "renormalized" interfaces. In particular, for interactions of the exponential form defined in Section 8 it is possible to classify the different phase diagrams which occur close to the $\sigma = 0$ end of the first-order transition separating the α and β phases. There are for these interactions a relatively small number of possibilities: a simple triple point, singular-continuous and quasicontinuous endpoints, and, in case A in the notation of Section 4, either a complex web of first-order transitions (with an infinite number of triple points) or an upsilon point, "regular" or "inverse." An upsilon point turns out to be an accumulation point of other upsilon points connected through a web of singular-continuous transitions in a sort of fractal structure.

While the exponential form of interaction may seem to be rather restrictive, it applies in a fairly general sense in Frenkel–Kontorova models provided the interfaces are widely separated. As this condition is satisfied in case A near the end of the first-order α–β transition (as can be seen in the pair approximation of Section 4), we believe that our description should be valid very near an upsilon point in one of these models. One can in fact check that the exactly soluble model of Aubry *et al.*[16] exhibits upsilon points in agreement with what we find in Section 8. Numerical studies[13,14] of Frenkel–Kontorova models in which harmonics are added to the cosine potential are also consistent with the picture of upsilon points presented here, though the precision is not very great. In addition, numerical studies of Frenkel–Kontorova models with nonconvex interactions[15,20–23] provide examples of triple points and quasicontinuous endpoints as well as upsilon points. We do not know of any examples

which could be interpreted as an inverse upsilon point or as accumulations of triple points of the type which occurs in case A with $t_{\alpha\beta}t_{\beta\alpha} < 0$, Section 8.

Our analysis is not limited to Frenkel–Kontorova models, and we would expect that similar phenomena would occur in the phase diagrams of three-dimensional ANNNI and chiral clock models. Thus far they have not (so far as we know) been observed, but that could simply reflect the fact that the phase diagrams are not very well understood in the intermediate temperature regime where the singular-continuous transitions occurring just beneath the critical temperature become transformed into the first-order structures which can be described (to some extent) by low-temperature series. These phenomena should also be accessible in experimental systems, though we know of no examples which have been observed up to the present time.

APPENDIX A: MINIMIZING (2.14)

Let H and N be real-valued functions of a set of parameters, collectively denoted by τ, satisfying the following conditions: there are real numbers $B > 0$, C, and D such that

$$N(\tau) \geqslant B > 0 \tag{A.1}$$

$$H(\tau) + CN(\tau) \geqslant D \tag{A.2}$$

for all τ.

Theorem. (a) The quantity

$$F = \inf_{\tau} [H(\tau)/N(\tau)] \tag{A.3}$$

is finite.

(b) The quantity

$$\Omega(f) = \inf_{\tau} [H(\tau) - fN(\tau)] \tag{A.4}$$

is finite for $-\infty < f < F$, and possibly on a longer interval. Where it is finite, $\Omega(f)$ is concave and monotone strictly decreasing as a function of f.

(c) If

$$\Omega(f) = 0 \tag{A.5}$$

has a solution, the unique solution is $f = F$. If there is no solution, then $\Omega(F)$ is positive, and $\Omega(f)$ is $-\infty$ for $f > F$.

Before beginning the proof, we note that $f = F$ is always the solution of (A.5) in the sense of being the (unique) point where the graph of $\Omega(f)$ crosses the abscissa, provided that in the case in which $\Omega(F)$ is positive, the graph is extended in an obvious way by dropping a vertical line to $-\infty$ at $f = F$.

To prove (a), use the fact that (A.1) and (A.2) yield lower bounds of $-C$ and $-C + D/B$ for H/N in the cases $D \geqslant 0$ and $D < 0$, respectively. For (b), use (A.1) and (A.3) to show that

$$\Omega(F) \geqslant 0 \tag{A.6}$$

Strict monotonicity of $\Omega(f)$ is a consequence of (A.1) whenever Ω is finite, and (A.6) shows that Ω is finite for all $f \leqslant F$. Concavity is a consequence of taking the infimum of a collection of affine ("linear") functions. Finally, for part (c), note that (A.3) and (A.1) imply that for any $\varepsilon > 0$, $\Omega(F + \varepsilon)$ is negative (possibly $-\infty$). Thus, either $\Omega(F) = 0$, and this zero is unique by strict monotonicity, or else $\Omega(F + \varepsilon)$ is $-\infty$, by concavity.

In applying these theorems to (2.14), the parameters of interest are the l_i and the m_i; note that i takes on a finite number of values. Condition (A.2) is not hard to check, assuming a reasonable behavior of the ϕ's. Note that H itself will not be bounded below if ε_α or ε_β is negative.

APPENDIX B: LOCATION OF POINTS IN THE PHASE DIAGRAM IN THE THREE-INTERFACE APPROXIMATION

The locations of various points in the phase diagrams in Fig. 12 are given in Table II, using the variables

$$a = (\bar{l} - l)\,\eta_\alpha + \phi_\alpha(\bar{l}) - \phi_\alpha(l) \tag{B.1}$$

$$b = (\bar{m} - m)\,\eta_\beta + \phi_\beta(\bar{m}) - \phi_\beta(m) \tag{B.2}$$

which are shifted and rescaled versions of η_α and η_β, respectively. The special values

$$a^+ = \phi_\alpha(l, m) + \phi_\beta(m, l) - \phi_\alpha(\bar{l}, m) - \phi_\beta(m, \bar{l}) \tag{B.3}$$

$$a^- = \phi_\alpha(l, \bar{m}) + \phi_\beta(\bar{m}, l) - \phi_\alpha(\bar{l}, \bar{m}) - \phi_\beta(\bar{m}, \bar{l}) \tag{B.4}$$

$$b^+ = \phi_\alpha(l, m) + \phi_\beta(m, l) - \phi_\alpha(l, \bar{m}) - \phi_\beta(\bar{m}, l) \tag{B.5}$$

$$b^- = \phi_\alpha(\bar{l}, m) + \phi_\beta(m, \bar{l}) - \phi_\alpha(\bar{l}, \bar{m}) - \phi_\beta(\bar{m}, \bar{l}) \tag{B.6}$$

Table II. Location of Points in the Phase Diagrams in Fig. 12

Point	a	b
$[lm]:[\bar{l}m]:[l\bar{m}]$	a^+	b^+
$[\bar{l}\bar{m}]:[\bar{l}m]:[l\bar{m}]$	a^-	b^-
$[\bar{l}m]:[lm]:[\bar{l}\bar{m}]$	a^+	b^-
$[l\bar{m}]:[lm]:[\bar{l}\bar{m}]$	a^-	b^+
$[l\bar{m}\bar{l}m]:[lm]:[\bar{l}m]$	a^+	$b^+ - \Delta^2\phi_\beta$
$[l\bar{m}\bar{l}m]:[l\bar{m}]:[\bar{l}\bar{m}]$	a^-	$b^+ - \Delta^2\phi_\alpha$
$[l\bar{m}\bar{l}m]:[lm]:[l\bar{m}]$	$a^+ - \Delta^2\phi_\beta$	b^+
$[l\bar{m}\bar{l}m]:[\bar{l}m]:[\bar{l}\bar{m}]$	$a^+ - \Delta^2\phi_\alpha$	b^-
$[lm\bar{l}\bar{m}]:[lm]:[\bar{l}m]$	a^+	$b^+ - \Delta^2\phi_\alpha$
$[lm\bar{l}\bar{m}]:[l\bar{m}]:[\bar{l}\bar{m}]$	a^-	$b^+ - \Delta^2\phi_\beta$
$[lm\bar{l}\bar{m}]:[lm]:[l\bar{m}]$	$a^+ - \Delta^2\phi_\alpha$	b^+
$[lm\bar{l}\bar{m}]:[\bar{l}m]:[\bar{l}\bar{m}]$	$a^+ - \Delta^2\phi_\beta$	b^-

give the locations of the upper (a^+), lower (a^-), right (b^+), and left (b^-) vertical and horizontal solid lines of superdegenerate points. Note that

$$a^+ - a^- = b^+ - b^- = \Delta^2\phi_\alpha + \Delta^2\phi_\beta \tag{B.7}$$

where $\Delta^2\phi_\alpha$ and $\Delta^2\phi_\beta$ are abbreviations for $\Delta^2\phi_\alpha(lm)$ and $\Delta^2\phi_\beta(ml)$ defined in (5.3) and (5.4). A three-phase point is identified in the table by specifying the three phases which come together at the point; thus $[l\bar{m}]:[lm]:[\bar{l}\bar{m}]$ is the point at the lower right end of the first-order (dashed) line in Fig. 12b. The corresponding points in the σ, ε plane are obtained using (5.5) and $\varepsilon = \eta_\alpha - \eta_\beta$.

APPENDIX C. CLOSED-FORM EXPRESSIONS FOR VARIOUS QUANTITIES USED IN SECTIONS 6 AND 7 AS SUMS OF Φ'S

We use the abbreviated notation for the ϕ's introduced after (2.11): subscripts are omitted, and the argument of each ϕ is a string of letters. If S and T are two such strings, ST is the combined string in which the letters of T follow those of S, and Sl and $S\bar{l}T$, etc., have an obvious significance. An *allowed* string is one in which l's and m's (possibly with bars) alternate. In order to be able to write sums such as (C.1) in a reasonably compact notation, it is convenient to adopt the convention that $\phi(S)$ vanishes if S is the *null string* with no letters, and $\phi(ST)$ vanishes if ST is not an allowed string, as is the case, for example, when S ends and T begins with an m.

We can then write (6.5) and (6.7) in the form

$$\Delta H = (\bar{l} - l)\,\varepsilon_\alpha + \sum_{C,\ C' \subset [lm]} \{\phi(C\bar{l}C') - \phi(ClC')\} \tag{C.1}$$

$$(l+m) f_0 = 2\sigma + l\varepsilon_\alpha + m\varepsilon_\beta + \sum_{C \subset [lm]} \phi(C) \tag{C.2}$$

where the sum over $C \subset [lm]$ includes the null string, and each distinct finite string of successive letters occurring in the infinite configuration $\ldots lmlm\ldots$, precisely once. While the null string can be omitted in (C.2), as the corresponding ϕ vanishes, it is essential in (C.1).

To obtain $W(L_1, L_2, \ldots, L_n)$ in closed form, first construct the corresponding string S; see (6.11) and the remarks which follow. This S, which we also denote by S_a, begins and ends with an $\bar{l}$. Changing the final $\bar{l}$ to l, the first $\bar{l}$ to l, or both yields the strings S_c, S_d, and S_b, respectively. That is, S_a, S_b, S_c, and S_d represent the central portions of the corresponding configurations (between the dashed lines in Fig. 16) used in the reconnection formula. Consequently, the exact formula for W is

$$W(L_1, L_2, \ldots, L_n) = \sum_{C,\ C' \subset [lm]} \{\phi(CS_aC') + \phi(CS_bC') - \phi(CS_cC') - \phi(CS_dC')\} \tag{C.3}$$

The approximation using a double difference, as in (6.9) and (6.11), comes from retaining only the single term in which C and C' are both null strings. (Formulas giving $\tilde{W}$'s in terms of W's are given in Appendix D.)

Formulas (7.11) and (7.12) take the form

$$\psi_\alpha = \sum_{A \subset [\bar{l}m]} \phi(A) \tag{C.4}$$

$$\psi_\beta = \sum_{B \subset [l\bar{m}]} \phi(B) \tag{C.5}$$

in the notation introduced above. To obtain a formula for some $\tilde{\phi}$, first construct the string T consisting of l's and m's (with or without bars) obtained by putting together the segments of the phases $\tilde{\alpha}$ and $\tilde{\beta}$ specified by the arguments of $\tilde{\phi}$ in the appropriate order. That is, T is the string obtained by removing the first and last letters of S in (7.16). The reconnection procedure then yields the formula

$$\tilde{\phi} = \pm \Bigg\{ \sum_{A,\ A' \subset [\bar{l}m]} \phi(ATA') + \sum_{B,\ B' \subset [l\bar{m}]} \phi(BTB') - \sum_{A \subset [\bar{l}m]} \sum_{B \subset [l\bar{m}]} [\phi(ATB) + \phi(BTA)] \Bigg\} \tag{C.6}$$

where the plus sign is employed if $\tilde{\phi}$ has an odd number of arguments, as in (7.15), corresponding to the interaction of an even number of $\tilde{\alpha}\tilde{\beta}$ interfaces, and the minus sign if $\tilde{\phi}$ has an even number of arguments.

To obtain an expression for Δ_σ, (7.20), in closed form, first write (7.17) as

$$\Delta H = (l - \bar{l})\,\varepsilon_\alpha + \sum_{A,\ A' \subset [\bar{l}m]} \sum \{\phi(AlA') - \phi(A\bar{l}A')\} \tag{C.7}$$

Next equate this with (7.18), use (C.6) with $T = l$ to provide an explicit expression for $\tilde{\phi}_\beta(\tilde{m}^*)$, and use (7.10) to write the result as

$$2\tilde{\sigma} = \bar{l}\tilde{\varepsilon}_\alpha + \bar{m}\tilde{\varepsilon}_\beta - 2\sigma - \bar{l}\varepsilon_\alpha - \bar{m}\varepsilon_\beta + \Delta_\sigma \tag{C.8}$$

with

$$\begin{aligned}\Delta_\sigma = &- \sum_{B \subset [l\bar{m}]} \phi(B) + \sum_{A \subset [\bar{l}m]} \sum_{B \subset [l\bar{m}]} [\phi(AlB) + \phi(BlA)] \\ &- \sum_{A,\ A' \subset [\bar{l}m]} \sum \phi(A\bar{l}A') - \sum_{B,\ B' \subset [l\bar{m}]} \sum \phi(BlB')\end{aligned} \tag{C.9}$$

One can show that (C.8) is equivalent to (7.19), and (C.9) can be rewritten in the more compact and symmetrical form

$$\begin{aligned}\Delta_\sigma = &\sum_{A \subset [\bar{l}m]} \sum_{B \subset [l\bar{m}]} [\phi(AmlB) + \phi(BlmA)] \\ &- \sum_{A,\ A' \subset [\bar{l}m]} \sum \phi(A\bar{l}A') - \sum_{B,\ B' \subset [l\bar{m}]} \sum \phi(B\bar{m}B')\end{aligned} \tag{C.10}$$

APPENDIX D: EXPRESSIONS FOR $\tilde{E}_D$ AND $\tilde{W}_k$, Section 6

Combining (6.3) and (6.15) yields the formula

$$\tilde{H}_D = H_D - N(f_L - f_0) \tag{D.1}$$

In the state $[L]$ there are no $\bar{L}$-type defects, so $\tilde{H}_D = 0$, and thus, using (6.4), one obtains the expression

$$\begin{aligned}L(f_L - f_0) &= E_D + W(L) + W(LL) + W(LLL) + \cdots \\ &= E_D + \sum_{\Gamma \subset [L]} W(\Gamma)\end{aligned} \tag{D.2}$$

in a notation in which subscripts have been dropped from the W's and commas have been omitted from their arguments, just as in the case of the ϕ's in Appendix C.

To obtain $\tilde{E}_D$, note that it is the change in $\tilde{H}_D$ if a single L in $[L]$ is changed to an $\bar{L}$, thereby changing N by $\Delta N = \bar{L} - L$, and H_D by

$$\begin{aligned}\Delta H_D &= W(\bar{L}) - W(L) + W(L\bar{L}) + W(\bar{L}L) - 2W(LL) + \cdots \\ &= \sum_{\Gamma,\ \Gamma' \subset [L]} \{W(\Gamma\bar{L}\Gamma') - W(\Gamma L\Gamma')\} \end{aligned} \tag{D.3}$$

with a notation parallel to that in Appendix C: the sum over Γ is over strings of L's of arbitrary length, starting with zero. Consequently, in view of (D.1),

$$\tilde{E}_D = -(\bar{L} - L)(f_L - f_0) + \sum_{\Gamma,\ \Gamma' \subset [L]} \{W(\Gamma\bar{L}\Gamma') - W(\Gamma L\Gamma')\} \tag{D.4}$$

with $f_L - f_0$ given by (D.2).

The $\tilde{W}$'s are obtained from the W's using reconnection formulas. A given set of arguments $\tilde{L}_1, \tilde{L}_2, \ldots, \tilde{L}_n$ specifies a corresponding string of L's and $\bar{L}$'s beginning and ending with $\bar{L}$, which we denote by $S = S_a$, while S_c, S_d, and S_b are obtained by omitting the first, the last, and both bars, respectively, from S. The formula for $\tilde{W}$ is then

$$\tilde{W} = \sum_{\Gamma,\ \Gamma' \subset [L]} \{W(\Gamma S_a \Gamma') + W(\Gamma S_b \Gamma') - W(\Gamma S_c \Gamma') - W(\Gamma S_d \Gamma')\} \tag{D.5}$$

ACKNOWLEDGMENTS

We thank L. M. Floria for helpful discussions. The National Science Foundation has provided support for this research through grants DMR-8613218 and DMR-9009474.

NOTE ADDED IN PROOF

A referee kindly brought to our attention the paper of F. Vallet, R. Schilling, and S. Aubry[24] which uses methods similar in spirit to those of Fisher and Szpilka[17] to calculate finite temperature properties of one-dimensional incommensurate structures.

REFERENCES

1. R. Blinc and A. P. Levanyuk, eds., *Incommensurate Phases in Dielectrics. 1. Fundamentals. 2. Materials* (North-Holland, Amsterdam, 1986).
2. P. Bak, *Rep. Prog. Phys.* **45**:587 (1982).

3. V. L. Pokrovsky and A. L. Talapov, *Theory of Incommensurate Crystals* (Harwood, New York, 1984).
4. H. Z. Cummins, Experiental studies of structurally incommensurate crystal phases, *Phys. Rep.* **185**:211 (1990).
5. W. Selke, *Phys. Rep.* **170**:213 (1988).
6. J. Yeomans, in *Solid State Physics*, Vol. 14, H. Ehrenreich and D. Turnbull, eds. (Academic Press, New York, 1988), p. 151.
7. D. G. Sannikov, in *Incommensurate Phases in Dielectrics*, Vol. 1, R. Blinc and A. P. Levanyuk, eds. (North-Holland, Amsterdam, 1986), p. 43.
8. T. Janssen, in *Incommensurate Phases in Dielectrics*, Vol. 1, R. Blinc and A. P. Levanyuk, eds. (North-Holland, Amsterdam, 1986), p. 67.
9. S. Aubry, *J. Phys.* (Paris) **44**:147 (1983).
10. S. Aubry, in *Structures et Instabilités*, C. Godrèche, ed. (Editions de Physique, Les Ulis, France, 1985), p. 73.
11. S. Aubry and P. Y. Le Daeron, *Physica D* **8**:381 (1983).
12. R. B. Griffiths, in *Fundamental Problems in Statistical Mechanics VII*, H. Van Beijeren, ed. (North-Holland, Amsterdam, to appear).
13. W. Chou and R. B. Griffiths, *Phys. Rev. B* **34**:6219 (1986).
14. K. Sasaki and L. M. Floria, *J. Phys. Cond. Mat.* **1**:2179 (1989).
15. K. E. Bassler, Ph.D. Dissertation, Carnegie-Mellon University, Pittsburgh, Pennsylvania (1990).
16. S. Aubry, F. Axel, and F. Vallet, *J. Phys. C* **18**:753 (1985).
17. M. E. Fisher and A. M. Szpilka, *Phys. Rev. B* **36**:644 (1987).
18. K. Sasaki, to be published.
19. L. H. Tang and R. B. Griffiths, *J. Stat. Phys.* **53**:853 (1988).
20. C. S. O. Yokoi, L. H. Tang, and W. Chou, *Phys. Rev. B* **37**:2173 (1988).
21. W. Chou, *J. Stat. Phys.* **50**:207 (1988).
22. M. Marchand, K. Hood, and A. Caillé, *Phys. Rev. Lett.* **58**:1660 (1987); *Phys. Rev. B* **37**:1898 (1988).
23. M. Marchand and A. Caillé, *Phys. Rev. B* **38**:4845 (1988).
24. F. Vallet, R. Schilling, and S. Aubry, *J. Phys. C* **21**:67 (1988).